
Article:
Michelbach, CA orcid.org/0000-0001-6448-2705 and Tomlin, AS orcid.org/0000-0001-6621-9492 (2021) Influence of Iso-Butanol Blending with a Reference Gasoline and Its Surrogate on Spark-Ignition Engine Performance. Energy and Fuels. ISSN 0887-0624

https://doi.org/10.1021/acs.energyfuels.1c01619

The Influence of Iso-Butanol Blending with a Reference Gasoline and its Surrogate on Spark-Ignition Engine Performance

Christian A. Michelbach*, Alison S. Tomlin

School of Chemical and Process Engineering, University of Leeds, Leeds LS2 9JT, United Kingdom

Keywords: Butanol, gasoline surrogate, spark-ignition, engine knock, downsized engine, turbocharging, biofuels.

Abstract: This study investigated the ability of a five-component gasoline surrogate (iso-octane, toluene, n-heptane, 1-hexene and ethanol) to replicate the combustion and knocking behaviour of a reference gasoline (PR5801 – RON 95.4, MON 86.6), under pressure boosted spark-ignition engine conditions at various levels of blending with iso-butanol. The ability of the neat surrogate was first evaluated for stoichiometric air/fuel mixtures, at an intake temperature and pressure of 320K and 1.6 bar, respectively, and an end of compression pressure of 30 bar, over a range of spark discharge timings. Throughout this regime, the surrogate was found to produce a good representation of the gasoline, particularly in terms of mean engine cycle properties, knock onsets and knock intensities. This high degree of similarity between the surrogate and gasoline was also seen previous rapid compression machine work, at comparable end-gas temperatures

(Michelbach, C.; Tomlin, A. An Experimental and Kinetic Modelling Study of the Ignition Delay and Heat Release Characteristics of a Five Component Gasoline Surrogate and Its Blends with Iso-Butanol within a Rapid Compression Machine. *Int. J. Chem. Kinet.* **2021**, *53* (6), 787–808. https://doi.org/10.1002/kin.21483). However, significant differences were observed between the cyclic variability of surrogate and gasoline results, which was attributed to compositional differences between the two fuels. This study also investigated the impact of iso-butanol blending (at ratios of 5-70% iso-butanol by volume) on the performance of the gasoline at knocking and non-knocking conditions, as well as the ability of the surrogate to replicate the observed blending behaviour, at the same experimental conditions. In general, increasing the iso-butanol volume was shown to decrease the knocking propensity of the fuel, except for a non-linear cross-over behaviour witnessed for 5% and 10% iso-butanol blends, wherein the 5% blend became less reactive than the 10% blend due to the heavy suppression of NTC behaviour in the 10% blend. Even at such low concentrations, iso-butanol appears to act as a strong radical sink, as identified by brute-force sensitivity analysis of predicted knock onsets. This is consistent with the findings of the aforementioned rapid compression machine study. Blends of 20-50% iso-butanol were found to be optimal for use in SI engines, providing considerable anti-knock benefits and comparable indicated power to gasoline, with blends of 20-30% being the most viable due to the lower quantities of biofuel required. Under blending with iso-butanol the surrogate continued to perform well but blends were observably less reactive than the corresponding gasoline blends at spark advance timings <8 CA° before top dead centre. The consistency found between trends within literature sourced rapid compression machine measurements and engine data presented in this study highlight the proficiency of fundamental

measurements in predicting combustion behaviour within an engine at similar thermodynamic conditions.

Table of Contents

1 Introduction 5

2 Methodology 11

2.1 LUPOE-2D Research Engine 11

2.2 Operating Procedure 16

2.3 Data Collection and Analysis 20

2.4 Engine Modelling 25

3 Results and Discussion 27

3.1 Surrogate Performance During Normal Combustion 27

3.2 The Influence of Iso-butanol on Normal Combustion Behaviour 32

3.3 Surrogate Performance During Knocking Combustion 39

3.4 The Influence of Iso-butanol on Engine Knock 45

4 Conclusions 59

5 Author Information 62

6 Supporting Information 62

7 Acknowledgements 63

8 References 64

1 Introduction

Currently, there is increased interest in the knocking behaviour of alternative fuels, such as biofuels and their blends with conventional fossil fuels, due to the growing need increase the renewable proportion of liquid transport fuels and consequently to lower greenhouse gas (GHG) emissions[1–4]. Renewable energy targets set out in the Renewable Energy Directive II (RED II)[5], published by the European Union (EU), dictate that by 2030, renewables must contribute at least 14% to the energy mix for all road and rail transport in the EU. The RED II favours the contributions of advanced biofuels to this target by limiting the contributions of unsustainable first-generation biofuels (such as those produced from food crops), and specifying a required minimum contribution for advanced biofuels of 3.5% by 2030[5]. Advanced alcohol biofuels are often considered as viable replacements or supplements for conventional fossil fuels, due to their potential to enhance the octane rating of fuels and their similar chemical and physical properties, making them compatible with modern spark-ignition (SI) engines (particularly when utilised as blended fuels)[6,7]. Ethanol is commonly blended at low concentrations with gasoline (5-10% volumetrically) for use in SI engines. The use of higher ethanol concentrations without engine modification is limited however, due to ethanol's relatively low energy density (which limits fuel efficiency), hydrophilic behaviour (which causes storage issues), and corrosivity (which can lead to the corrosion of engine components and fuel supply infrastructure)[8–10]. Alternatively, the butanol isomers show promise as potential transport fuels in spark ignition (SI) engines. They have higher calorific values than ethanol, are not as hydrophilic, have a lower vapour pressure and can be blended to higher ratios in a conventional SI engine without the risk of corrosion[11,12]. Of the butanol isomers which may be produced as an advanced biofuel, iso-butanol has been identified as potentially having the greatest octane boosting qualities, with relevance to use in SI engines[13].

Engine downsizing is an emerging SI engine technology which utilises pressure boosting (through the use of turbocharging or supercharging) to produce smaller, more fuel-efficient engines with the power capabilities of a larger conventional SI engine. However, the degree of pressure boosting, and thus the effectiveness of downsized engines, is limited by the problem of engine knock[1]. Conventional engine knock is initiated by the compression of unburnt gases during the combustion process by the propagating flame front, to temperature and pressure conditions high enough to accelerate chemical reactions in the unburnt gas, leading to autoignition[14]. This autoignition induces sonic pressure waves which further interact with the flame front, producing high frequency pressure oscillations within the engine cylinder, which interact with the cylinder surfaces. This causes the cylinder to vibrate, producing an audible ping, and potentially causing serious damage to the cylinder and piston head[14–16]. Engine knock and autoignition behaviours are dependent on the fuel composition and the evolution of thermodynamic conditions during engine operation, and are governed chemical kinetics[17]. A thorough understanding of potential alternative fuels, their anti-knocking quality and auto-ignitive behaviour is required to facilitate the sensible use of such fuels in modern SI engine technologies. However, ignition and SI performance studies for alternative fuels such as iso-butanol and blends with gasoline in SI engines are uncommon[18–22], and studies of blends at boosted engine pressure conditions are even less common in the literature. There is therefore a need to determine the influence of iso-butanol blending on boosted SI engine performance and knocking behaviour.

Full characterisation of the combustion behaviour of alternative fuels (such as iso-butanol and gasoline blends), for application to the diverse range of SI engine technologies present in the transport fleet, requires detailed investigation at an exhaustive range of conditions. Performing

such analysis experimentally would require a prohibitive amount of time, potentially limiting the introduction of viable alternative fuels into the transport energy sector. Computer modelling provides an opportunity to predict combustion behaviour relatively cheaply and quickly, and probe conditions where experimental measurements are difficult or impossible[23,24]. If models are to be developed for the accurate and consistent prediction of combustion behaviour within SI engines, simple surrogate fuels are needed which provide a robust representation of the combustion behaviour of chemically complex gasolines, both as 'neat' fuels and under blending with biofuels[25]. While there are many rapid compression machine (RCM) studies which test the fidelity of gasoline surrogate fuels[26–30], studies within SI engines are less common[31,32], while studies of low temperature pressure boosted SI engines are rarer still[3]. In the study of Khan et al.[33], the ability of a primary reference fuel (PRF) and toluene reference fuel (TRF) to represent the knocking behaviour of gasoline was evaluated within a normally aspirated SI engine. The investigated TRF provided a reasonable representation of the gasoline at a spark advance timing of 20 CA° bTDC (before top dead centre) but the PRF was significantly more reactive than the reference gasoline and the TRF, while displaying a larger degree of variability. Modelling predictions made for more complex four component surrogates showed that a surrogate designed to match the composition of the reference gasoline, in terms of matching iso-paraffin, n-paraffin, aromatic and naphthene concentrations, predicted knock onsets (KN) closest to those witnessed for gasoline within an SI engine[33]. In the study of Sarathy et al.[31], the ability of seven and eight component surrogates were investigated with respect to FACE-F and FACE-G gasolines, which were designed to match various octane quality parameters and physical properties of the reference gasolines[34]. Both surrogates were capable of accurately capturing the knock intensity (KI) trends within a cooperative fuel research (CFR) engine at RON-like and MON-like

conditions, with the eight-component surrogate providing the best representation of the reference gasoline[31]. These previous studies display the importance of matching the broad chemical composition of gasoline in replicating knocking behaviour. In this study, the ability of a five-component surrogate (5-C) to replicate the combustion and knocking behaviour of the reference gasoline within an SI engine is investigated, as previous surrogates of lower degrees of complexity have proven ineffective under these conditions[3,35,36]. By limiting the surrogate to five components, the computational burden of any future engine modelling will be minimised when compared to more complex surrogates such as those investigated by Sarathy et al.[31].

The effect of oxygenate blending with various gasolines and their surrogates has been shown in the literature to produce complex responses in the octane quality of the resultant fuels. In the case of ethanol, Hunwartzen[37] originally reported a linear by volume increase in RON during the blending of ethanol and gasoline. A similar response was also shown for the blending of iso-butanol with gasoline in the same study. However, both of the alcohols were shown to produce a non-linear MON response to increasing oxygenate volumes, showing an antagonistic effect at blends below very high concentrations (80% by volume) of the corresponding alcohols. Later work by Anderson et al.[38]contradicted the ethanol blending trends shown in the work of Hunwartzen[37], showing a linear by mole blending response instead, and in subsequent work demonstrating the existence of non-linear blending regimes[39]. This non-linear octane quality response (in terms of both RON and MON) was confirmed in the study of Foong et al.[40], which showed the effects of ethanol blending to vary between synergistic and antagonistic, depending on the composition of the base gasoline surrogate. PRF, and the associated iso-octane and n-heptane components, were shown to blend synergistically with ethanol, with the RON of blends of ethanol and iso-octane occasionally exceeding the RON of ethanol. On the other hand, the

addition of toluene (to produce a TRF surrogate) displayed an antagonistic effect of ethanol blending. Foong et al.[40] also showed that increasing the fraction of toluene in TRFs of constant RON resulted in an increasingly linear blending response, indicating that the effects of toluene and ethanol blending were in competition with the synergism shown in the blending of ethanol with iso-octane and n-heptane. This highlights the importance of representing the aromatic and paraffinic fractions of the reference gasoline accurately within a surrogate, such that these complex blending behaviours will be represented. This may also provide an explanation for the different blending responses shown in the literature for ethanol blending, as the distribution of components varies between different gasolines. The linear and non-linear blending regimes for ethanol blending with TRF mixtures were comprehensively investigated in the study of AlRamadan et al.[41], which produced an octane prediction model consisting of linear and non-linear by mole regions. With regards to engine knock, the role of ethanol in blending with hydrocarbon fuels as a radical scavenger (or radical sink) for reactive OH radicals has been shown in previous studies to supress the low temperature chain branching of hydrocarbon fuels, delaying autoignition and therefore engine knock onset[40,42]. Similarly, the role of n-butanol as a radical scavenger when blended with n-heptane[43,44] and TRF surrogates[2,4,45] has been described in the literature. However, when blended with TRF, n-butanol produced an antagonistic IDT response within RCM experiments, causing autoignition to occur earlier for blends of 20% n-butanol than the base TRF and its reference gasoline, within the negative temperature coefficient region[4]. Recent studies on the blending of iso-butanol with gasoline and it's surrogates by Goldsborough et al.[46] and Michelbach and Tomlin[47] identified the role of iso-butanol as a radical sink during low temperature oxidation, increasing the fuels resistance to auto-ignition in this region, as well as the promoting role of the fuel at higher temperatures, due to an increase in

hydrogen abstractions from the tertiary iso-butanol sites. Non-linear blending was also apparent in the study of Michelbach and Tomlin[47], which showed an antagonistic effect of iso-butanol blending on IDTs at low iso-butanol concentrations (5-10%).

Fan et al.[48] investigated the anti-knock influence of all four butanol isomers on a PRF and TRF, for blends of 0-50% butanol by volume, by making RON measurements with a CFR engine. The butanols produced an increase in knock resistance for all blends, with the order of greatest anti-knock boost being iso-butanol > sec-butanol > n-butanol > tert-butanol, for blends with PRF and iso-butanol > sec-butanol > tert-butanol > n-butanol for TRF blends. RON measurements were correlated with IDTs measured at 770 K and 20 bar and this condition was selected for further chemical kinetic analysis, again highlighting the role of iso-butanol in the suppression of low temperature reactivity, with the hydrogen abstraction of butanol by OH radicals playing an important role in this process. Han et al.[49] further investigated the combustion of gasoline surrogate blends (PRF and TRF) with the butanol isomers within an optical GDI engine, at blends of 30% butanol. This work showed that butanol addition caused a reduction in peak cylinder pressures, heat release rates, and the speed of flame propagation, while extending the duration of combustion. The charge cooling effect of butanol addition was highlighted as the driving physical reason for this behaviour, combined with the chemical kinetic influence of butanol of bulk reactivity. Jesu Godwin et al.[50] investigated the impact of iso-butanol blending with gasoline for a four-stroke SI engine, using blends of 10% iso-butanol by volume. This showed a peak cylinder pressure and crank angle of peak pressure for the 10% iso-butanol blend which was similar to that of the unblended gasoline, indicating that the charge cooling influence of iso-butanol blending may not be significant at such low concentrations.

This study aims to characterise the influence of iso-butanol on SI engine performance by blending iso-butanol with a reference gasoline and its surrogate, at blending ratios of 5-70% iso-butanol by volume. The behaviour of these blends under knocking and non-knocking ('normal') combustion is investigated experimentally within a pressure boosted single cylinder research engine, as is the ability of the surrogate to replicate iso-butanol blending behaviour.

2 Methodology

2.1 LUPOE-2D Research Engine

The Leeds University Ported Optical Engine, Mk II with a disc-shaped combustion chamber (LUPOE-2D) is capable of achieving the high end of compression pressures required to investigate combustion under modern SI engine conditions relevant to downsized, turbo-charged engines, as seen in various previous works[3,51,52]. The LUPOE-2D currently features a disc-shaped cylinder head, with a centrally located spark (consisting of a 0.5 mm steel anode, housed in a 3 mm diameter alumina sheath), to minimise the impact of turbulence and facilitate the generation of uniform in-cylinder fluid flow. This configuration is not typical of common SI engines (which often utilise a significantly off-centre spark location) and may impact on the likelihood of engine knock within the LUPOE-2D, relative to an otherwise identical engine. A centrally located spark will, when compared to an off-centre spark location, produce a faster burn rate and thus a shorter combustion time. While a shorter combustion time would intuitively decrease the likelihood for knock to occur (as it provides less time for the unburnt gas to auto-ignite)[53,54], the increased pressure and temperature of the unburnt gas, due to the increased burn rate, will increase the chance of knock occurring[55–58]. Therefore, the central spark plug location employed in this study is not expected to limit the ability of the LUPOE-2D to generate knocking combustion. To further reduce the impact of turbulence effects, such as "swirl" and "tumble"[36], to two

diametrically opposed, rectangular shaped ports provide intake for the combustion cylinder. Each intake port is inclined by 20% with respect to the cylinder interior. A singular exhaust duct interacts with the bulk test gas via a void between the cylinder barrel and cylinder liner. This liner contains two rings of circular exhaust holes (of 10 mm diameter each), which allow for the test gas to exit to the exhaust via the cylinder void. Port opening for fuel intake and exhaust outtake is controlled by piston motion, which will block the access to exhaust holes and fuel intake ports during motoring. This ported breathing behaviour generates an in-cylinder flow field which is uniform, such that the LUPOE-2D can be described as a 'featureless flow engine'[59]. The engine is motor driven, with motion provided by a dynamometer and electric motor, which can be controlled to allow the LUPOE-2D to operate at varying engine speeds. The engine can operate regularly at stable engine speeds of 400-2000 RPM, typically within a variation of -15 to +30 RPM at an engine speed of 750 RPM and -30 to +50 RPM for an engine speed of 1500 RPM. A flywheel is fitted to the engine driveshaft, storing rotational kinetic energy during the operation of the engine, which limits the influence of fast angular velocity fluctuations due to combustion and the resultant differences in compression and expansion strokes. Engine parameters are listed in table 1.

Table 1. LUPOE-2D design specifications**.**

Parameter	**Value**
Cylinder Head Shape	**Disc**
Effective Compression Ratio (CR_{EFF})	**11.5**
Dynamic Compression Ratio (CR_{DYN})	**15.2**
Bore	**80 mm**
Stroke Length	**110 mm**

Clearance Height	**8 mm**
Connecting Rod Length	**232 mm**
Inlet Ports Opening/Closure	**107.8 CA°**
Exhaust Ports Opening/Closure	**127.6 CA°**

It should be noted that there are significant differences between the design and operation of the LUPOE-2D and a conventional SI engine. Principally, the LUPOE-2D operates on a skip-firing basis, reducing the influence of residual gases and heating on subsequent combustion cycles. In this sense, the firing-cycle conditions within the LUPOE-2D should be similar to those of an RCM, wherein the presence of post-combustion residuals is ideally eliminated, allowing for a direct comparison of combustion behaviours between the two facilities and providing useful data for future model evaluation. The inlet/exhaust architecture is also substantially different between the LUPOE-2D and a conventional SI engine, to facilitate a combustion environment free of the influence of turbulence. This allows for the isolation of iso-butanol concentration as the main contributing variable influencing SI engine performance and knocking behaviour, as the influence of turbulence is beyond the scope of this study. During operation, the LUPOE-2D in-cylinder pressure reaches as high as 30 bar before ignition, with peak temperatures prior to ignition typically in the range of 620 – 630 K[59], similar to those conditions typical of a downsized pressure boosted SI engine.

Typically, the LUPOE-2D requires at least 1.6 L (two 800 ml tanks, one for line flushing and the other for engine testing) of liquid fuel for the completion of a single experiment (one fuel blend at a range of crank-angle spark advance timings). Due to the large quantities of fuel required, small errors in the measurement of individual liquid components do not strongly influence the

ignition properties of the final blended fuel. As such, liquid fuel mixtures are prepared as 4 L batches, ensuring a consistent mixture between fuel line flushing and experiments, with a reserve of mixture for the completion of repeats/further experiments. Each individual liquid component is measured volumetrically, using a graduated measuring cylinder appropriate to the required volume of the liquid component. Each measuring cylinder corresponds to an individual fuel for the duration of the mixture preparation process and all glassware is thoroughly cleaned between the preparation of different fuel batches. Fuel is supplied from an 800 ml fuel tank to the LUPOE-2D by a standard automotive filter and electrical pump system. The mass flow rate of liquid fuel is controlled by an M53 Bronkhorst Coriolis mass controller and fuel pressure is maintained at 3 bar by a Bosch pressure regulator. Combustion air is supplied to the LUPOE-2D at a pressure of 4 bar, by two separate supply lines, each controlled by a Bronkhorst EL-FLOW thermal mass flow meter, with a maximum mass flow rate of 33 g/s, and feedback adaptation to maintain a constant air/fuel ratio during operational pressure fluctuation. To further minimise the influence of air flow oscillations during LUPOE-2D operation, a 5 L surge tank is installed between each inlet pipe and mass flow controller, ensuring a consistent air supply pressure. Air temperature is maintained at the required value by a series of five 175 W and 200 W band heaters along the length of each intake pipe, which also provides the heat flux required to vaporise liquid fuels during mixing with the combustion air. Fuel in injected 350 mm upstream of the cylinder intake port, wherein it mixes with the combustion air, via a venturi carburettor, ensuring the full vaporisation of liquid fuel prior to entering the cylinder. For all experiments, the cylinder is preheated to a temperature of 323 K, for a period of at least 120 minutes. Due to the large thermal inertia of the cylinder and the effectiveness of the 50 W cartridge heaters, pre-heating to higher temperatures is not feasible. Increased pre-heat temperatures would also impact

the engine resting time between each run, as the cylinder must be left to cool substantially in the absence of an active cooling system. A 3D schematic of the LUPOE-2D engine layout and a detailed 2D schematic of the air/fuel system are shown in figure 1.

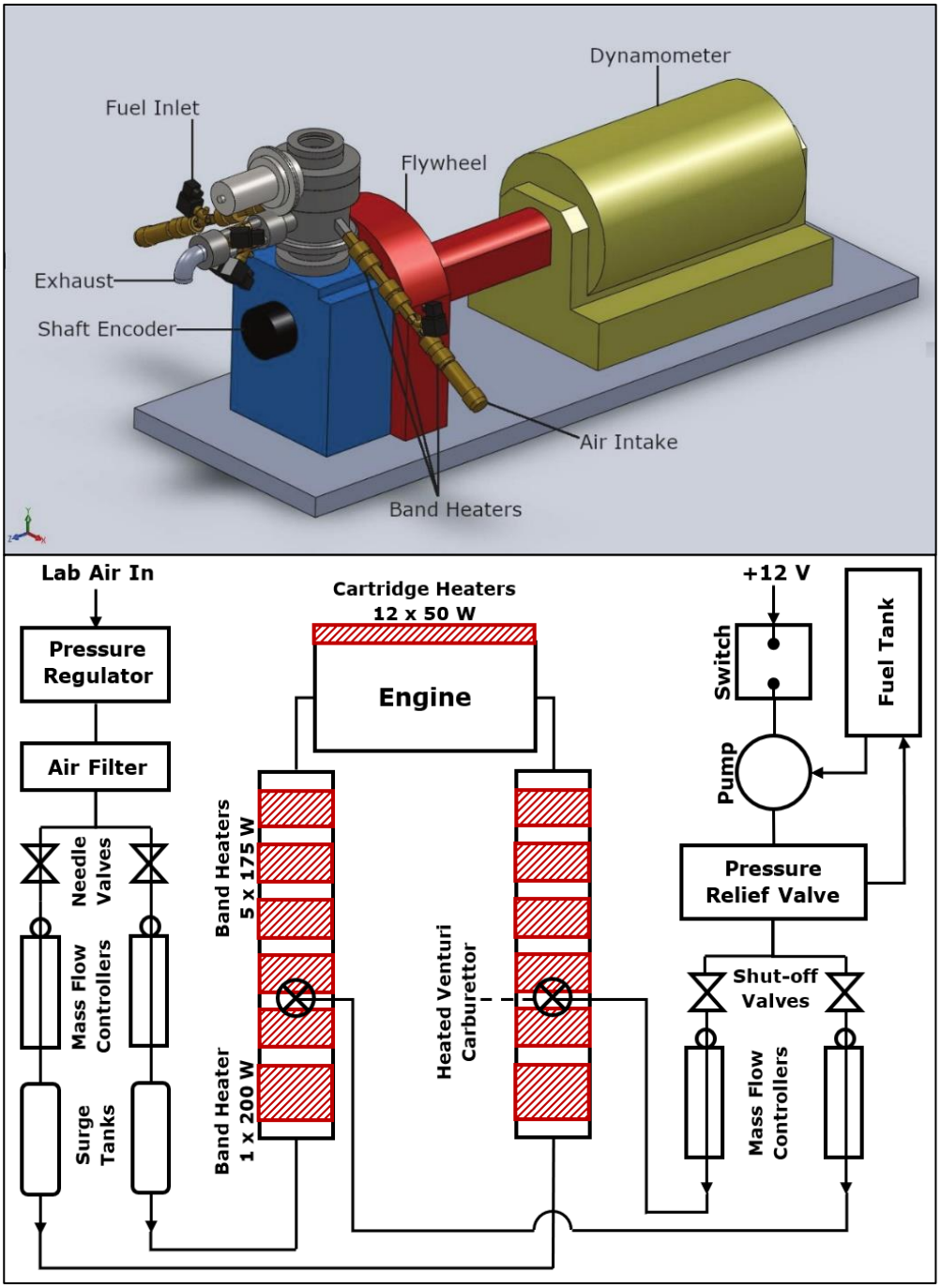

Figure 1. A labelled 3D schematic of the LUPOE-2D engine and detailed 2D schematic of the air/fuel system.

2.2 Operating Procedure

A wide range of iso-butanol blending ratios were investigated within this study, spanning 0-70% by volume iso-butanol blending with both gasoline and 5-C. This includes blends of 5, 10, 20, 30, 50 and 70% iso-butanol (iB05, iB10, iB20, iB30, iB50, iB70), giving a total of 14 investigated fuel blends. These same blending ratios were previously investigated within the University of Leeds RCM at boosted SI engine relevant conditions[47], allowing for a comparison between the two sets of data. The 5-C surrogate utilised has been formulated to closely match the PR5801 reference gasoline (supplied by Shell Global Solutions) in terms of RON, MON, hydrogen to carbon (H/C) ratio and molecular composition. A reference gasoline containing an ethanol fraction typical of that available 'at the pump' (particularly E5 fuel in the United Kingdom) was chosen for this study, as it provides an opportunity to investigate the SI engine performance of potential advanced biofuel blends containing multiple oxygenated components (in this case, ethanol, and iso-butanol). As mentioned previously, the EU RED II[5] mandates the use of increased quantities of advanced biofuels within the transport energy mix. Variety in the biofuel component palette may provide useful for meeting these requirements, particularly in cases where it is more economically or environmentally viable to produce one particular biofuel from a given feedstock, or in cases where multiple biofuel components can be produced through a single process. With the requirement for advanced biofuels in the energy mix set to increase in the near future[5], it is necessary to understand the combustion behaviour of such fuels and their surrogates. The gasoline surrogate applied in this study contains components of iso-octane, n-heptane, toluene, 1-hexene and ethanol to represent the broad composition of the reference

gasoline in terms of paraffins (iso- and n-paraffins), aromatics, olefins, and alcohols (ethanol). Further details regarding the 5-C surrogate are given in the study of Michelbach and Tomlin[47], while the compositions and comparative properties of the surrogate and reference gasoline can be seen in table 2. Previous RCM IDT measurements of this reference gasoline, its surrogate, and their respective blends with iso-butanol have shown a good degree of agreement between gasoline and surrogate blends, throughout the investigated regime[47]. The 5-C and gasoline IDTs showed a percentage difference well within 10% of gasoline IDTs throughout most of the relevant regime (710-870 K), with the exception of the 740 K case, due to a somewhat shallower NTC of the 5-C. When blended at 10 and 30% iso-butanol by volume the degree of representation was similar (all within 15%), with the exception of iB30 also at 740 K. Blending to higher concentrations of iso-butanol (50 and 70%) showed significant IDT differences at the lowest investigated temperatures of 710 and 740 K, but these are less relevant for the investigation of knock in the LUPOE-2D, particularly when the increased autoignition resistance of these blends. When measured at a range of conditions, IDT measurements can be used to identify the autoignition response of the fuel to changing thermodynamic conditions, as opposed to the specific standard conditions of RON and MON measurements, making IDT measurements (and the associated IDT response profiles) a more expansive descriptor of a fuels autoignition behaviour. This is particularly true under pressures and temperatures which are representative of pressure boosted (such as the LUPOE-2D) or low temperature combustion engines, as historical fuel parameters such as RON and MON cannot capture fuel reactivity under such conditions[60–63]. As the development of SI engines pushes operational regimes even further from those of the RON and MON tests, the utility of such tests and their relevance to modern engines will continue to decline[62–64]. IDT measurements at specific temperature and pressure conditions have

previously been correlated with bulk octane quality parameters, as seen in the literature[62,65–68]. However, it is acknowledged that due to differences in the evolution of the end gas between fundamental systems (RCM) and reciprocating engines, IDTs may not be exactly equivalent to RON measurements[69,70].

Table 2. A comparison of the compositions and properties of reference gasoline (PR5801) and the 5-C surrogate.

Gasoline PR5801 Component	**Gasoline PR5801** (vol%)	**5-C Surrogate Component**	**5-C Surrogate** (vol%)
Paraffins	**47.1**	iso-Octane	**50.5**
		n-Heptane	**10.8**
Aromatics	**26**	Toluene	**25.9**
Naphthenes	**8.2**		
Olefins	**7.9**	1-Hexene	**8.1**
Ethanol	**4.7**	Ethanol	**4.7**
Other Oxygenated Compounds	**4.4**		
Average Molecular Composition	**$C_7H_{13.5}O_{0.15}$**		**$C_{6.8}H_{12.9}O_{0.1}$**
RON	**95.4**		**95.1**
MON	**86.6**		**87**
H/C	**1.93**		**1.9**
Octane Sensitivity	**8.8**		**8.1**
AKI	**91**		**91.05**

For all investigated conditions, the LUPOE-2D is operated at an engine speed (ω) of 750 RPM, an initial pre-heat temperature (T_i) of 323 K, a boosted pressure (P_i) of 1.6 bar and a stoichiometric air/fuel ratio. A list of experimental parameters, as applied throughout this study, is shown in table 3. To avoid the presence of post-combustion residuals and exhaust gases, reducing the likelihood of preignition, 24 skip-firing cycles (of which 16 were fuelling cycles) were completed between every firing cycle. This was shown to be effective in previous LUPOE-2D studies[3,36]. Starting at a spark advance crank angle of 2 CA° bTDC, each fuel is tested for a minimum of 13 sequential firing cycles (with 24 skip-firing cycles between each firing cycle). The engine is then left to cool ambiently (without a source of active cooling) for 30 minutes before the next experiment can begin. Spark discharge timing is then advanced by a maximum of 2 CA° and the process is repeated. Once knocking conditions are identified as oscillations in the recorded in-cylinder pressure history and as a characteristic audible "ping", spark advance timing is iterated by 1 CA° in either direction to locate the condition at which knock first occurs. Spark discharge timing is then advanced by 1 CA° until the knock limited spark advance is found, as defined by the latest spark advance timing which generates a minimum of 90% knocking cases[59]. The spark advance timing may then be advanced further, up until the maximum safe peak pressure of 120 bar is achieved.

Table 3. LUPOE-2D operating parameters during all test conditions.

Parameter	**Value**
Engine Speed (ω)	**750 RPM**
Intake Temperature (T_{in})	**323 K**
Intake Pressure (P_{in})	**1.6 bar**
Equivalence Ration (Φ)	**1.0**

Air Mass Flow Rate ($\dot{m}_{air}$)	**10.2 g/sec**
Exhaust Gas Recirculation (EGR)	**0 %**

2.3 Data Collection and Analysis

The LUPOE-2D employs bespoke control and data collection systems. A DsPIC 6140A microcontroller provides triggering signals for inlet and exhaust valve timing, spark firing and data acquisition, as a function of shaft encoder clock signals. Instructions are provided to the microcontroller via a C script, which can be easily modified to change experimental parameters (such as spark advance timing and the number of motoring and fuelling cycles), while an in-circuit debugger (MPLAB ICD 3) provides on-the-fly debugging and programming of the microcontroller. Operation of the LUPOE is initiated by an electronic trigger, which activates the microcontroller and relevant instructions. Experiments are automatically terminated by the control system after a given number of firing cycles to reduce the likelihood of extreme knocking conditions, which may cause damage to the equipment or pose a safety risk. Furthermore, the incorporation of real-time pressure signal detection allows for LUPOE-2D to be immediately and automatically terminated, should in-cylinder pressures exceed a pre-determined safety threshold.

During operation, the in-cylinder pressure is measured using a combination of two pressure transducers: a dynamic pressure transducer (a piezoelectric 0-250 bar Kistler 601A), which is mounted flush to the cylinder wall, and an absolute pressure transducer (0-20 bar Kistler 4045 A20), which is mounted 60° below TDC, at the lower end of the piston barrel. During piston motion, the position of the absolute transducer is such that it is isolated from the combustion chamber as the piston passes a crank angle of 58.6° bTDC, where in-cylinder pressures are typically 2.5-3 bar. Voltage signals from the absolute pressure transducer are amplified by a Kistler 4601A piezoresistive amplifier with a voltage output of 0-10 V, providing a reference

pressure for the calculation of the cylinder pressure. The dynamic pressure transducer can be used to measure rapid pressure changes during the experiment, the signals of which are amplified by a Kistler 5007 charge amplifier with a voltage output also of 0-10 V. Analogue pressure signals for the absolute and dynamic pressure transducers are converted to digital signals and then read by a National Instruments 6110 and DIO-32HS, respectively, sampling at a rate of 200 kHz. Crank angle position during LUPOE-2D operation is measured by a Horner 3202 shaft encoder, which produces 1800 encoder pulses per revolution (plus an additional pulse for TDC), providing a sampling resolution of 0.2 CA° (a sampling rate of 22.5 kHz at an engine speed of 750 RPM). No corrections are made to account for varying piston speed during the engine cycle. Higher resolution pressure data is resampled with respect to the lower resolution crank angle data for analysis, with the influence of signal noise being adequately removed through the application of a second order Savitzky-Golay filter, with a window of 0.6 CA°.

The calculation for cylinder pressure (P_{cy}), requires the gauge pressure (P_g), absolute pressure (P_a) and the crank-angle degrees at exhaust port closure (Φ_{EC}):

$$P_{cy} = P_g + \left(P_a(\emptyset_{EC}) - P_g(\emptyset_{EC})\right) \qquad \textbf{Equation 1}$$

where the P_g is provided by dynamic pressure transducer measurements and P_a is provided by absolute pressure transducer measurements.

The knocking behaviour of a given fuel can be described by its knock onset (KN) and knocking intensity (KI)[15], where KN describes the crank angle location at which autoignition of the end gas occurs, producing observable engine knock. The methods described in the work of Liu and Chen[71] can be applied to determine these parameters analytically. This method defines the point of KN as the point at which the first significant pressure inflection is observed in the pressure

trace, which leads to a series of pressure oscillations. The point of inflection can be calculated precisely by the rate of change of the pressure-crank angle gradient ($\mathrm{KN} = -\frac{dP^2}{d\theta^2}$).

From this, the knock onset can be determined by finding the first point at which KN exceeds a pre-determined knock threshold. This threshold should be less than the maximum amplitude of the knock oscillations but also greater than the amplitude of the noise caused by engine vibrations. Selecting a single knock threshold for all cases may lead to the misidentification of knocking cases, due to the influence of characteristic engine non-uniformities and the resultant cyclic variability. Therefore, a varying knock threshold is selected after an initial visual inspection of pressure traces, which involved the location of a clear peak in the second pressure derivative prior to a series of oscillations, on a case-by-case basis, typically with values of 15-30 bar/CA°^{2}. A similar approach has been applied in a previous LUPOE-2D study to account for cyclic variability in the determination of KN, utilising a varying threshold value of 20-30 bar/CA°^{2} (again based on the visual inspection of pressure traces)[3], and has also been shown to produce KNs within 0.2 CA° of onsets determined by direct imaging of combustion[59]. The lower varying threshold boundary chosen in this study (when compared to literature thresholds[3,71]) facilitates the detection of relatively weak knocking cases identified during the analysis of recorded pressure data. KI is defined as the maximum amplitude of the rate of pressure rise. An example of the results derived through this method can be seen in figure 2.

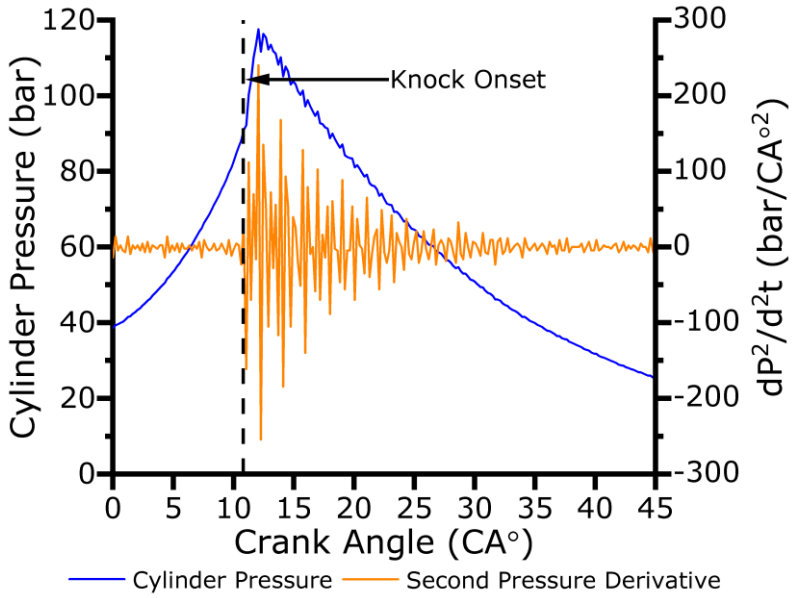

Figure 2. An example of the KN analysis performed in this study, showing the cylinder pressure history, rate of pressure gradient change history and the point of knock onset. This example shows a knocking case for gasoline, at a crank angle spark advance timing of 10 CA° bTDC.

Heat release rates and predictions of gas temperature can be extracted from experimental pressure traces. These provide an opportunity to analyse combustion behaviour and observed blending phenomena quantitatively, as well as providing additional targets for model evaluation. By applying the first law of thermodynamics, the ideal gas law, and assuming the cylinder charge is a single zone, the gross heat release per crank angle during combustion ($dQ_{hr}/d\theta$) can be given by equation 2**.**

$$\frac{dQ_{hr}}{d\theta} = \frac{\gamma}{\gamma-1} P_{cy} \frac{dV}{d\theta} + \frac{1}{\gamma-1} V \frac{dP_{cy}}{d\theta} - \frac{dQ_{ht}}{d\theta} \qquad \textbf{Equation 2}$$

Here, γ is the temperature dependent ratio of specific heats for the air/fuel mixture, V is the cylinder volume, and $dQ_{ht}/d\theta$ is the heat transfer between the gas and the cylinder wall (heat loss), which may be described as shown in equation 3.

$$\frac{\mathrm{d}Q_{ht}}{\mathrm{d}\theta} = hA(T_g - T_w) \qquad \textbf{Equation 3}$$

Here, h is the heat transfer coefficient, A is the combustion chamber internal surface area, and T_g and T_w are the gas and wall temperatures, respectively.

The Cantera [72] Python library and a combined iso-butanol/gasoline surrogate mechanism consisting of the Sarathy et al. butanol isomers mechanism [73] and Lawrence Livermore National Laboratories (LLNL) "Gasoline Surrogate" mechanism [74] (detailed in the previous work of Michelbach and Tomlin[47]) is applied for the calculation of heat release rates in this study, to calculate the temperature dependent specific heats at each crank angle step. Specific heats for each species are determined using the NASA 7-coefficient polynomial parameterisation, as dictated by mechanism thermodynamic data.

Cycle-to-cycle variations in peak pressure are typical during LUPOE-2D operation and can provide insight into cyclic variability and the prevalence of engine knock at a given condition. The coefficient of variation (CoV) is a property which characterises these variations and can be defined as the ratio of peak pressure standard deviation to the mean peak pressure. In this study, the mean peak pressure (as well as other mean properties given) is calculated as the average of each individual peak pressure, based on an ensemble of 24 recorded combustion cycles for each case. Similarly, the CoV for the crank angle location of peak pressure can also be defined in this manner and provides an opportunity for further investigation of the cyclic variability and knocking propensity at a given condition. This statistical parameter is often applied to evaluate cyclic variability within engine studies[7,51,75–77].

2.4 Engine Modelling

To simulate the evolution of the gas within the cylinder during combustion, a multi-zone zero-dimensional SI engine model is applied, using CHEMKIN-PRO[78], to predict unburned gas temperatures, LTHR and gas composition as it is compressed by the advancing flame front. These analyses are applied within this study to correlate unburned gas temperatures within the SI engine to end of compression temperatures within an RCM (as seen in the parallel study[47]), as well as to enable discussion of the important kinetic features of iso-butanol blending with the surrogate through the application of a brute-force reaction rate sensitivity analysis. Correlating end gas temperatures between the two facilitates highlights the applicability of fundamental experiments and modelling (in the case of RCM work) to more complex systems, such as knocking combustion within the LUPOE-2D. This also allows for a discussion of RCM modelling sensitivity analysis in the context of SI engine phenomena, revealing the kinetic processes driving autoignition and blending behaviours. The SI engine model consists of two homogeneous zones, a burned and an unburned zone, separated by a turbulent premixed flame. At initialisation (intake valve closing time), the unburned gas contains only the gaseous air/fuel mixture, and the burned zone is empty. After combustion begins, reactants in the unburned zone are transformed into products in the burned zone by the flame sheet (assumed to be of negligible physical size). Full details of the model theory can be seen in the CHEMKIN-PRO[78] documentation[79]. Auto-ignition of the unburned gas is predicted by detailed chemical kinetics, utilising the combined iso-butanol/gasoline surrogates mechanism[47]. The mass exchange rate between the unburned and burned zone is specified by the mass fraction burned (MFB) profile of the median pressure cycle for each blend and spark advance timing condition. The median cycle is chosen over the mean cycle for this purpose to avoid the introduction of non-physical behaviour in the MFB profile. However, it should be noted that the median cycle introduces

other uncertainties, as the median cycle in terms of one parameter (such as peak pressure) is not necessarily the median cycle in terms of other parameters (such as the crank angle location of peak pressure), due to the nature of cyclic variability. For the simulation of knocking cases, pressure cycles which display knock at a given spark timing are isolated from non-knocking cycles and the median profile for only knocking cases is used as the basis for the calculation of MFB profiles. MFB can be calculated from experimental pressure data at each crank-angle via the application of equations 2 and 3 to account for heat losses during operation, normalised by the lower heating value of the fuel such that a prediction can be made for combustion efficiency, as shown in equation 4.

$$MFB = \frac{\int (dQ_{hr}/d\theta) d\theta}{m_f Q_{LHV}} \qquad \textbf{Equation 4}$$

Here, Q_{LHV} represents the lower heating value of the fuel and m_f is the fuel mass supplied per cycle. The degree of agreement produced by the applied engine modelling methodology with experimental work is shown in the example figure 3, for the representation of cylinder pressure and apparent heat release rate.

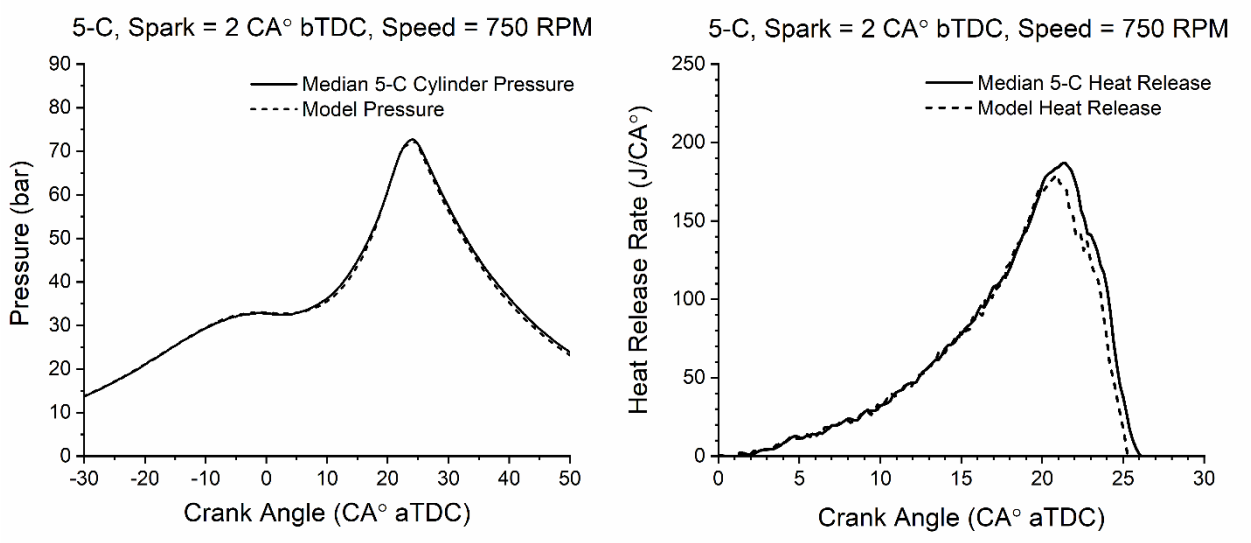

Figure 3. An example of the representation of the median experimental pressure cycle in terms of cylinder pressure and net heat release, for the median condition of 5-C, 2 CA° bTDC.

3 Results and Discussion

3.1 Surrogate Performance During Normal Combustion

Normal combustion is defined (within this study) as a combustion process wherein no anomalous engine phenomena can be observed, such as engine knock or pre-ignition. The ability of the 5-C surrogate to represent the behaviour of the reference gasoline under normal combustion is illustrated in figure 4a, which shows a comparison of the mean in-cylinder pressures for the two fuels at spark advance timings of 2, 4, and 6 CA° bTDC. Here any knocking cases have been removed prior to the calculation of the mean pressure cycle. For the 6 CA° cases, the influence of knock was minor and only three and four cycles were removed from a total of 24-26 firing cycles for the gasoline and 5-C, respectively. Therefore, the mean displayed in this case is a reasonable representation of the bulk behaviour of each fuel under normal combustion conditions. For a spark advance of 2 CA°, the surrogate represents the combustion behaviour of the gasoline well, closely matching the mean peak pressure (65.7 bar for both fuels), the crank angle location of the peak pressure (24.8 CA° for both fuels) and the evolution of the pressure increase. A similarly high degree of agreement can be seen at spark advance timings of 4 and 6 CA° bTDC. The work of Agbro et al.[3] investigated the representation of the same reference gasoline by a three component TRF surrogate, formulated from iso-octane, n-heptane and toluene. This previous study showed that the TRF produced a significantly lower peak pressure and pressure rise rate during normal combustion at a spark advance timing of 2 CA°. This indicates a lower burning velocity than the reference gasoline, as peak pressure may be applied as a proxy for the burning rate for fuels of comparable calorific values[3,51,52]. This behaviour was

attributed to the broad compositional differences between the TRF and gasoline. The utilised TRF contained a higher concentration of paraffins, particularly the relatively slow burning iso-octane, while containing no ethanol or olefinic components, which have been shown to have higher burning velocities than iso-octane and toluene[80]. The 5-C surrogate aims to replicate the volume fractions of ethanol, olefins, and aromatics in the reference gasoline, producing an accurate representation of the gasoline's burning rate and pressure evolution during normal combustion.

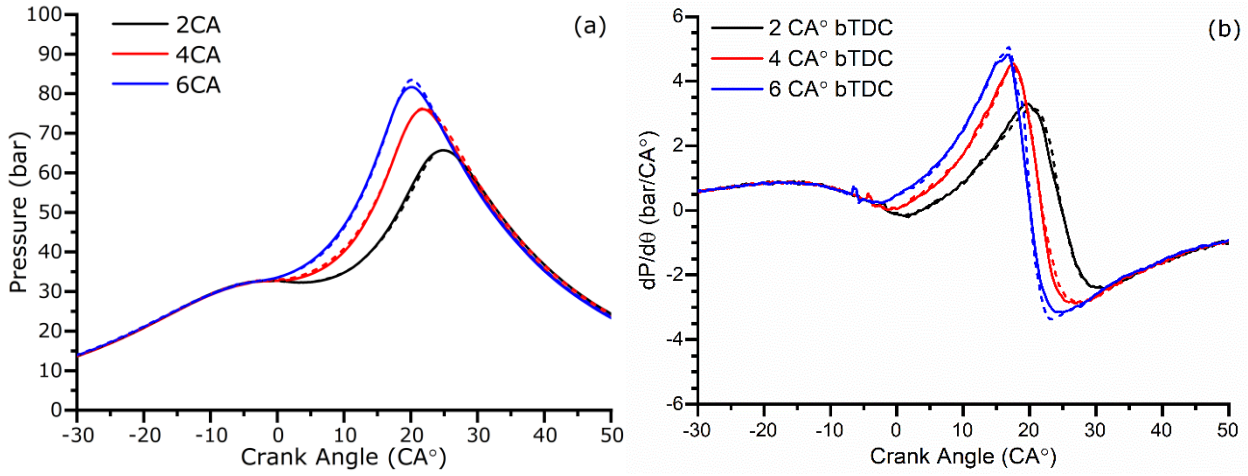

Figure 4. a) Mean in-cylinder pressure measurements under normal combustion, at spark advance timings of 2-6 CA°. b) First pressure derivatives for the mean pressure cycles of 5-C and gasoline, for normal combustion cases. Solid lines show mean 5-C values. Dashed lines show mean gasoline values.

While the normal combustion behaviour for the 6 CA° case is generally well represented, gasoline does display a slightly larger mean peak pressure (~2%) than the 5-C in this case. The crank angle location of these peak pressures is the same for each fuel (20.1 CA°), and the first pressure derivatives for each fuel only produce minor observable differences (figure 4b). While the difference in peak pressure is minor, it may be indicative of the lower octane sensitivity (*S*)

of the 5-C fuel (8.1 as compared to 8.8 for the reference gasoline). Post-spark unburnt gas temperatures increase as spark timing is advanced further from TDC[36], thus an advancement of spark timing from 4 CA° to 6 CA° bTDC would see a greater increase in reactivity for the more sensitive gasoline when compared to 5-C, as illustrated by a faster burning rate or a larger mean peak pressure for normal combustion conditions. Branched alkanes typically display slower burning velocities than straight chain alkanes of similar length. Therefore, the large fraction of iso-octane in the surrogate (more than the total of all paraffins in the reference gasoline) are a potential source of the observed burning rate differences. Also, the naphthenic content of the gasoline is not represented in the surrogate, which has been shown in the literature to produce similar burning velocities to straight chain alkanes[81,82]. Therefore, differences in the bulk burning velocity of the surrogate and the gasoline may exist, which become apparent at advanced spark timings. The burning velocity of a fuel affects the engine efficiency and the burn rate of the fuel, also impacting the peak pressure[83].

In general, as spark timing is advanced further from TDC, mean peak pressure increases, whereas the crank angle of this peak decreases, moving closer towards TDC. This increase in mean peak pressure can be attributed somewhat to the increase in unburnt gas temperatures as spark timing is advanced[36]. While the crank angle location of the mean peak pressure appears to move earlier in the cycle with respect to TDC, when investigated relative to the spark firing, the location is roughly constant between 4 and 6 CA° bTDC spark timing. This may be due to the removal of knocking cycles in the calculation of mean parameters at 6 CA° bTDC spark timing, which tend to occur in “fast” cycles. Fast cycles are defined as any firing cycle with a peak pressure greater than the mean peak pressure plus one standard deviation, whereas slow cycles

are the mean peak pressure minus a standard deviation. Similar definitions have been applied previously to characterise SI engine cycles in the literature[3,51,84,85].

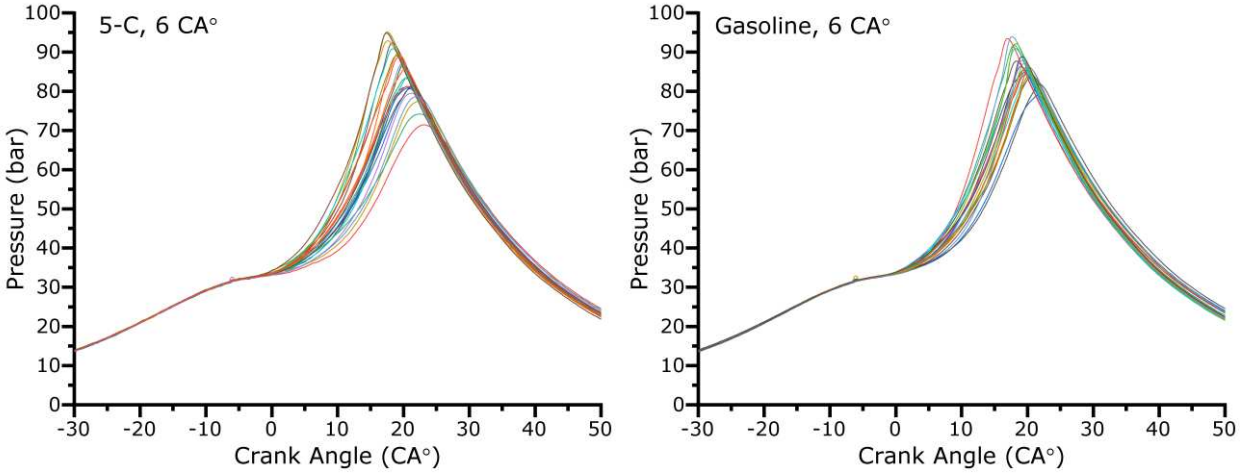

Figure 5. An example of the cycle-to-cycle variation for 5-C and gasoline normal combustion cases at a spark advance timing of 6 CA°.

SI engine spark timing is commonly optimised for the heat release profile of the most common cycle, therefore, 'real' engine performance (efficiency and power) can be negatively impacted by fuels which display a large degree of cyclic variability[15,51]. Furthermore, substantial cyclic variability (greater than 10% in terms of IMEP variability) causes a large degree of variability in engine speed, which is manifest as a noticeable deterioration in vehicle driveability[15]. Cyclic variability can be observed under nominally identical conditions due to variations in instantaneous rates of combustion between each cycle. Such variations may be due to a variety of potential sources[15,51,84,86], including mixture inhomogeneity within the cylinder (particularly near to the spark plug), spark discharge characteristics, 'trapped' fuel, residuals, and turbulence and charge motion during combustion. Examples of the cyclic variability for the 5-C and gasoline fuels, for normal combustion cases only at a spark timing of 6 CA° bTDC, can be seen in figure 5.

Table 4. Mean peak pressures and the associated crank angle locations for the normal combustion of gasoline and the 5-C surrogate, as well as the associated coefficients of variation. The crank angle change from ignition is the difference between the spark timing and the crank angle location of the peak pressure.

Fuel	**Spark Timing** (CA° bTDC)	**Mean Peak Pressure** (bar)	**Crank Angle Location** (CA° aTDC)	**CoV_{Pmax}** (%)	**Crank Angle Change from Ignition** (CA°)	**CoV_{CA}** (%)
Gasoline	**2**	**65.7**	**24.8**	**7.5**	**26.8**	**6.2**
	4	**76.3**	**21.9**	**6.9**	**25.9**	**5.7**
	6	**83.5**	**20.1**	**5.4**	**26.1**	**7.6**
5-C	**2**	**65.7**	**24.8**	**7.2**	**26.8**	**10.0**
	4	**76.1**	**21.9**	**7.3**	**25.9**	**6.7**
	6	**81.7**	**20.1**	**7.6**	**26.1**	**8.1**

The CoV of peak pressures and the associated crank angle locations are given in table 4 and describe the cyclic variability of 5-C and gasoline for each normal combustion case. At a spark advance timing of 2 CA°, the cyclic variability of peak pressure is similar for both 5-C and gasoline, with a slightly lower degree of variability for the surrogate. However, the degree of variability in the crank angle location of peak pressure is significantly higher for 5-C. A clear reduction can be seen in the cyclic variability of gasoline as the spark timing is advanced from 2 to 6 CA°, whereas the cyclic variability of 5-C increases. The 5-C also generally displays a higher degree of variability throughout the normal combustion regime, in terms of both the peak pressure and crank angle location of peak pressure. A possible source of this increased variability may be the large amounts of toluene (>25 % by volume) in the surrogate blend, which has been

shown to be sensitive to non-uniformities within temperature environments during RCM experiments[87]. During the completion of LUPOE-2D experiments, it was also observed that the use of large amounts of toluene led to the production of considerable carbon deposits on the interior surface of the engine cylinder. The presence of combustion residuals such as these are known to increase cyclic variability[15,51,84]. These findings limit the viability of surrogates composed of large quantities of toluene within SI engines. Morgan et al.[88] showed a reasonably good agreement between high toluene concentration surrogates and the reference gasoline in a HCCI engine. However, experience with such surrogates in the LUPOE-2D and the knowledge that toluene combustion can rapidly form multiple soot precursors[89–92], dictates that these surrogates would lead to an increased propensity for soot formation, and therefore cyclic variability. A large degree of cyclic variability can be observed for such surrogates in an SI engine in the study of Kalghatgi et al.[93]. Therefore, for a surrogate to accurately represent the cyclic variability of gasoline, the aromatic content of the gasoline should be considered as an important target during for surrogate formulation.

3.2 The Influence of Iso-butanol on Normal Combustion Behaviour

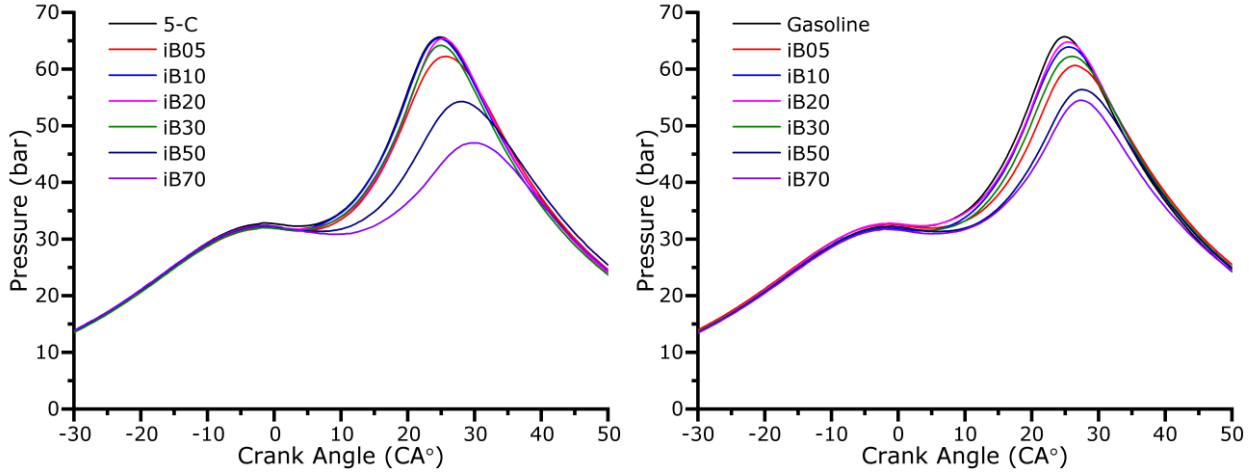

Figure 6. Mean pressure cycles for the normal combustion of iso-butanol blends with 5-C (left) and gasoline (right), at a spark timing of 2 CA° bTDC.

The influence of iso-butanol blending on the normal combustion of 5-C and gasoline within the LUPOE-2D can be seen in figure 6, which shows mean pressure cycles for each of the investigated blends, at a spark advance timing of 2 CA° bTDC. Interestingly, increasing the blending level of iso-butanol appears to induce a non-linear response in the mean peak pressure for blends with both 5-C and gasoline. This can also be seen in table 5. At these conditions, the addition of a small amount of iso-butanol appears to produce an observable decrease in the mean peak pressure and an increase in the corresponding crank angle location, as seen in the case of the 5% iso-butanol blends (iB05). As the volume fraction of iso-butanol is increased further to 10% (iB10), the mean peak pressure increases relative to iB05, and the mean crank angle location decreases. Generally, alcohols have been reported in the literature to display faster burning velocities than iso-octane and toluene (large components of the 5-C surrogate), which would be expected to produce an increase in the maximum pressure for fuels with similar calorific values[3,25,52,59,80,94]. In the literature, iso-butanol has been shown to produce laminar burning velocities similar to, but slightly faster than, those of gasoline, iso-octane and toluene, at similar conditions[95–98]. However, interpreting laminar burning velocities in the context of SI engine conditions can be uncertain, as highlighted in the works of Serras-Pereira et al.[99] and Aleiferis et al.[100]. These studies describe issues with interpreting such data due non-idealistic phenomena during engine combustion, such as turbulence, flame cellularity and changing temperatures and pressures. Aleiferis et al.[100] utilised a high speed to obtain images of flame growth within a direct injection SI research engine, for a RON 95 gasoline, iso-octane, ethanol, n-butanol, ethanol and methane. By doing this, the study was able to compare flame growth

speeds between the fuels, showing the order of the rate of flame growth to be ethanol > n-butanol > gasoline > iso-octane. While this study did not directly measure the flame growth speed of iso-butanol, based on the work of Gu et al.[101], it is expected to be similar to that of n-butanol at conditions relevant to the LUPOE-2D. At high pressures, Gu et al.[101], showed a cross-over in the laminar burning velocities of the butanol isomers, with iso-butanol displaying the fastest burning velocity at the highest investigated pressure of 0.8 MPa. Based on this knowledge, a blend of 5% iso-butanol would reasonably be expected to produce a slightly higher peak pressure than the 5-C and gasoline. However, this is not what is observed in the results of LUPOE-2D experiments.

In recent RCM work[47], the iB05 blends produced a significant reduction in low temperature heat release (LTHR) at the lowest investigated temperature of 710 K, when compared to 5-C, reducing the peak LTHR rate by approximately half. This suppression of LTHR at low temperatures may lead to a reduction in the charge heating of the end gas during normal combustion. While this process is beneficial in terms of a fuels knock resistance (by lowering the end gas temperature and pressure)[102–104], under normal combustion peak pressures may be reduced. However, this seems unlikely to be significant at spark advance timings so far from knocking timings. It would appear more probable that, despite efforts to isolate the charge cooling effects due to fuel evaporation through the use of port fuel injection in the LUPOE-2D, the endothermic evaporation of the iso-butanol fuel fraction is influencing in-cylinder temperature evolution during combustion. This can be attributed to a combination of the limited pre-heating temperature of 323 K for the equipment (including the air/fuel intake manifold) and iso-butanol's large enthalpy of vaporisation (45 kJ/mol at 358 K[105]), particularly compared to the enthalpy of vaporisation of iso-octane (31.7 kJ/mol at 358 K[106]), which makes up the bulk of the

surrogate. This evaporative charge cooling by small concentrations of iso-butanol is in direct competition with the higher burning rate. This can be seen in figure 7, which shows the mean heat release rate and bulk gas temperature profiles for blends of 5-C, iB05 and iB10, calculated from experimental pressure traces, as described in the methodology. The addition of even small amounts of iso-butanol has an apparent effect on both the evolution of the gas temperature and the peak temperature, which is contrary to the heat release analysis performed for a blend of 10% iso-butanol with gasoline by Jesu Godwin et al.[50], but is in agreement with the trends observed by Han et al.[49]. A mean peak temperature of 2400 K was achieved with the 5-C, whereas the addition of iso-butanol limited this peak temperature to 2320 K and 2260 K for the iB05 and iB10, respectively. This is indicative that some charge cooling is happening during testing, as if the initial temperature and pressure conditions were the same throughout testing, the higher burning velocity of the iso-butanol relative to the fuel components would be expected to increase the burning rate and therefore, the resultant maximum temperature would be greater than that of the 5-C (as combustion occurs within a smaller cylinder volume). The effect of charge cooling appears to be counteracted by an increase in heat release rate, as the iso-butanol content transitions from 5-10%, despite the lower gas temperatures, which indicates an increase in the burn rate. The interplay between these behaviours due to blending may warrant further research for the determination of optimal fuel blends and to investigate the feasibility of iso-butanol blends within direct injection SI engines, where charge cooling is more prevalent[107].

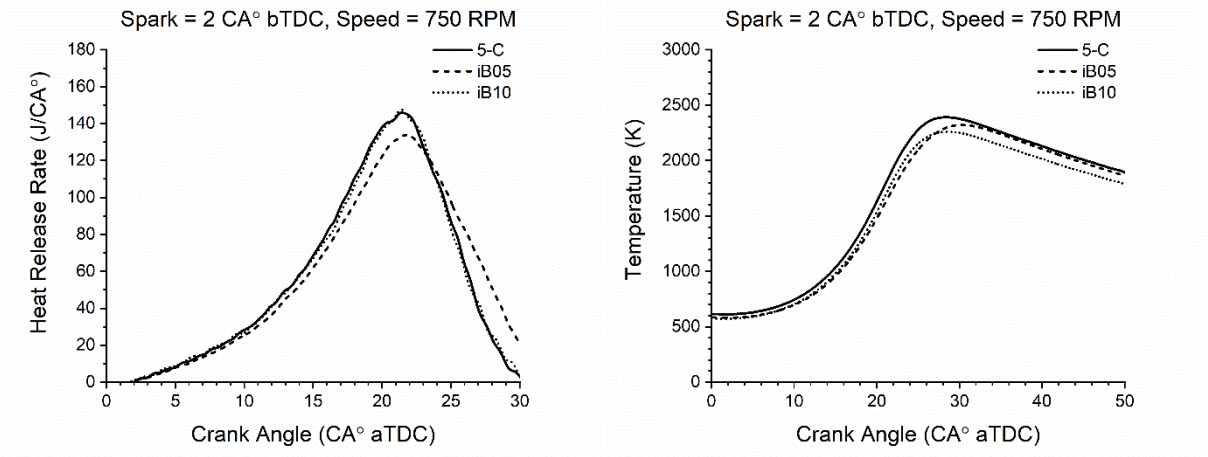

Figure 7. Heat release rates and temperature profiles for blends of 5-C, iB05 and iB10, at a spark advance timing of 2 CA° bTDC.

Mean peak pressures and crank angle locations for iB10 blends are similar to those displayed by the 5-C and gasoline fuels, as well as blends of 20% iso-butanol (iB20) by volume. This behaviour for the iB10 blends is similar to that seen in the SI engine study of Jesu Godwin et al.[50], which showed similar peak pressures and crank angle locations for gasoline and a 10% blend with iso-butanol. Previous studies of n-butanol blending with gasoline displayed similar behaviour for an investigated blend of 20% n-butanol[3,35,36]. Increasing the volume of iso-butanol further, to >30% of the fuels total volume (iB30-70), produces a clear reduction in the mean peak pressure, similar to that seen in the work of Han et al.[49]. At these large concentrations of iso-butanol, the decrease is likely due to the significant influence of the alcohol-component on the blends calorific value as well as the increased impact of iso-butanol charge cooling[49,108,109]. The lower calorific value of the blends is in competition with the increase in burning rate of the pure iso-butanol, as a faster burning rate means that combustion can be completed at smaller cylinder volumes, earlier in the piston stroke[3]. This explains the near constant mean properties of iB10 and iB20 before the decrease in mean peak pressures when the blending ratio is increased to iB30.

Table 5. Mean peak pressures and the associated crank angle locations of the peaks, for blends of iso-butanol with 5-C and gasoline at a spark timing of 2 CA° bTDC.

Base Fuel	**Iso-Butanol Content** (vol%)	**Mean Peak Pressure** (bar)	**CoV_{Pmax}** (%)	**Crank Angle Location** (CA° aTDC)	**CoV_{CA}** (%)
Gasoline	**0**	**65.7**	**7.5**	**24.8**	**6.2**
	5	**60.6**	**8. 8**	**26.6**	**10.0**
	10	**63.9**	**7.6**	**25.5**	**7.6**
	20	**64.8**	**7.8**	**25.5**	**6.8**
	30	**62.3**	**8.3**	**25.9**	**7.9**
	50	**56.4**	**10.5**	**27.3**	**8.0**
	70	**54.5**	**18.3**	**27.3**	**18.9**
5-C	**0**	**65.7**	**7.2**	**24.8**	**10.0**
	5	**62.3**	**10.4**	**25.5**	**9.7**
	10	**65.4**	**8.2**	**24.8**	**7.8**
	20	**65.4**	**5.9**	**25.2**	**5.2**
	30	**64.2**	**6.2**	**24.8**	**4.5**
	50	**54.3**	**17.1**	**28.1**	**11.7**
	70	**47.0**	**16.1**	**29.5**	**10.2**

While the representation of gasoline and iso-butanol blending trends is generally well captured by the surrogate, clear differences in the mean cycles of gasoline and 5-C iB50-70 blends are apparent in figure 6. Previous work which showed lower peak pressures during n-butanol blending with a TRF surrogate, when compared to gasoline blends, proposed that this behaviour

was due to the slightly lower calorific value of the surrogate when compared to gasoline, which was amplified as more of combustion volume becomes significant later in the piston cycle[3]. This may also be the case for 5-C blends of iB50 and iB70, which both display lower mean pressures than the gasoline equivalents at a later crank angle location, indicating more of the combustion process occurs at larger cylinder volumes. The significant reduction in mean peak pressures observed for large concentrations of iso-butanol would lead to a reduction in engine power for these blends, limiting their viability for use in SI engines at this spark timing. However, advancing spark timing further from TDC results in larger peak pressures and more engine power, providing that no knock occurs. An increase in the fuels knock resistance due to increased iso-butanol blending would facilitate the advancement of spark timing further, possibly allowing for engine powers comparable to those of gasoline.

Previous work investigating blends of gasoline and a TRF with n-butanol highlighted the ability of 20% n-butanol blending by volume to reduce cyclic variability within the LUPOE-2D[3]. However, this reduction of variability does not appear present in the blending of iso-butanol with gasoline, at blending ratios of 5-30% iso-butanol by volume, possibly due to the larger temperature sensitivity of iso-butanol reactivity in comparison with n-butanol, as seen in RCM IDT studies[2,4,13,47]. For large volumes of iso-butanol (iB50 and iB70), cyclic variability increases significantly for both peak pressure and the crank angle location of peak pressure. This carries negative implications for the use of such high butanol concentration blends within SI engines, as high degrees of cyclic variability are known to degrade engine performance and driveability[15,51]. An increase in cyclic variability for fuels of high iso-butanol concentration is a further indication of the impact of charge cooling by iso-butanol evaporation during the combustion process, despite efforts to eliminate the phenomena. It is necessary that potential alternative fuels target

the minimisation of cyclic variability, as well as improvements in knock resistance and engine power. In this regard, blends of 10-30% iso-butanol produce similar degrees of cyclic variability to the base gasoline.

3.3 Surrogate Performance During Knocking Combustion

For engine cycles which contain knock, the mean peak pressure is no longer a reliable proxy for the burning rate of the fuel due to the presence of autoignition[3]. However, for fuels with a similar burning rate (as determined through the investigation of normal combustion cases) the crank angle location of the peak pressure in knocking cycles may indicate the susceptibility of the fuel to autoignition. In this regard, while the crank angle location of peak pressure is largely similar for the gasoline and 5-C fuels at 6 and 8 CA°, the 5-C reaches a peak pressure 1.5 CA° earlier than gasoline at a spark timing of 10 CA° bTDC. However, in general the representation of the gasoline's mean pressure cycle development by the 5-C is good, with or without the inclusion of knocking cycles, as seen in figure 8 and table 6.

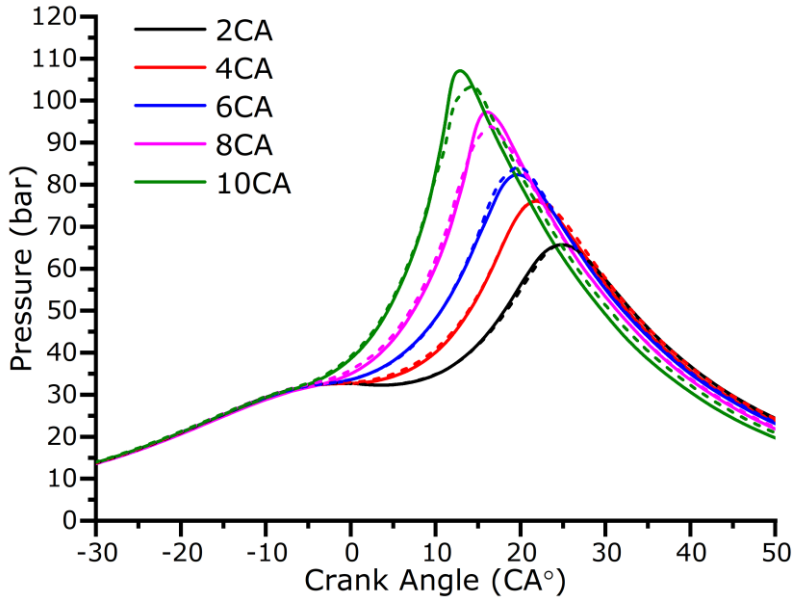

Figure 8. Mean in-cylinder pressure measurements for all combustion cases (normal and knocking), at spark advance timings of 2-10 CA°. Solid lines show mean 5-C pressures. Dashed lines show mean gasoline pressures.

Table 6. Mean peak pressures and the associated crank angle locations for the combustion (normal and knocking) of gasoline and the 5-C surrogate. The crank angle change from ignition is the difference between the spark timing (bTDC) and the crank angle location of the peak pressure (aTDC).

Fuel	**Spark Timing** (CA° bTDC)	**Mean Peak Pressure** (bar)	**Crank Angle Location** (CA° aTDC)	**CoV_{Pmax}** (%)	**Crank Angle Change from Ignition** (CA°)	**CoV_{CA}** (%)
Gasoline	**8**	**93.8**	**16.5**	**7.7**	**24.5**	**12.1**
	10	**103.4**	**14.4**	**5.9**	**24.4**	**13.5**
5-C	**8**	**97.3**	**16.2**	**4.5**	**24.2**	**8.1**
	10	**107.2**	**12.9**	**3.4**	**22.9**	**8.6**

An example of cyclic variation within knocking engine cycles can be seen in figure 9, at spark timings of 8 and 10 CA° spark advance timings for 5-C and gasoline fuels. At both conditions, the 5-C produces a significantly lower degree of cyclic variability than the corresponding gasoline cases. By observing the individual cycle pressure traces in figure 9, it would appear that this difference is due to the larger amount of slower gasoline cycles. This is contradictory to trends observed under normal combustion, wherein the 5-C typically displays a greater degree of cyclic variability. Similar behaviour has been witnessed in previous LUPOE-2D work[35], utilising the same reference gasoline and a TRF under a large degree of engine knock. Furthermore, this behaviour agrees with RCM IDT measurements for the 5-C[47], which showed a small degree of

experimental error (defined as twice the standard deviation) in IDT measurements at the intermediate to high temperature range (~740-870 K), indicating a high degree of repeatability in the induction of autoignition. As mentioned previously, cyclic variations within SI engines are an intrinsic phenomenon of engine combustion produced by an array of underlying reasons, which ultimately results in variations of in-cylinder pressure and unburnt gas temperatures. In this regard, the mechanism generating observable differences in measured engine behaviour (such as peak pressures and the associated crank angle locations) is similar to that driving variation within RCM measured IDTs. Such IDT variations are commonly attributed to uncertainties in the pressure and temperature within the combustion chamber at the EOC, when compared to predicted EOC conditions[110,111]. The degree of cyclic variability in peak pressure decreases as the spark timing is advanced further from TDC for both the gasoline and 5-C fuels, as shown by the CoV displayed in table 6. An increase can be observed in the CoV of the crank angle location of the peak pressure, when the spark timing is advanced from 8 to 10 CA° bTDC, despite an apparent reduction in the range and standard deviation of this value over all cycles, due to significant decrease in the mean location of peak pressure.

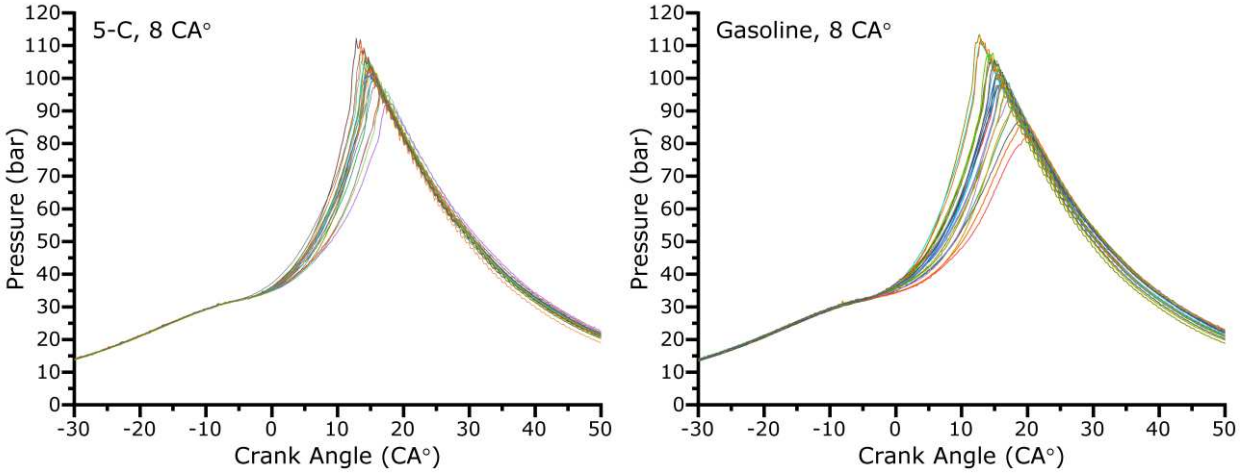

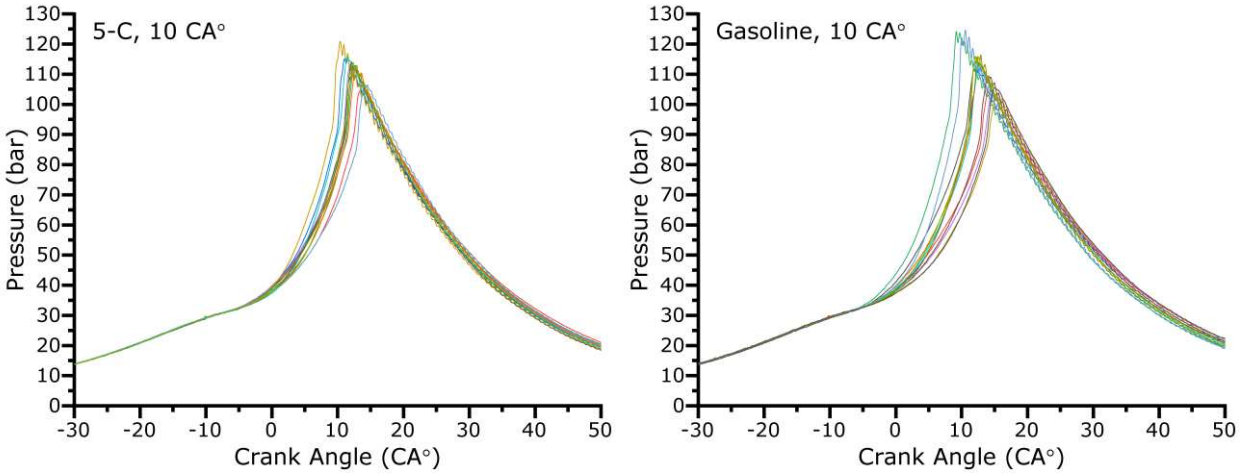

Figure 9. Examples of the cycle-to-cycle variation for 5-C and gasoline combustion cases, including prevalent knocking combustion, at a spark advance timing of 8 and 10 CA° bTDC.

Mean KNs and KIs are shown for spark timings of 6, 8 and 10 CA° bTDC in figure 10. In terms of these parameters, the 5-C gives an excellent representation of the reference gasoline within the LUPOE-2D, particularly at spark advance timings of 6 and 8 CA°, where KNs are near identical. This matches the behaviour observed in RCM IDT measurements, which also showed an excellent representation of the autoignition behaviour of the reference gasoline[47]. Small differences in RCM measured IDT times, such as 1-2 ms, may translate into differences as large as tens of crank angle degrees in SI engine KN. Therefore, the development of a surrogate that accurately matches both autoignition behaviour in an RCM and knocking propensity in an SI engine can be difficult. When compared to a previous TRF study[3], the 5-C produces a much better representation of the gasolines knocking propensity, particularly at a spark timing of 6 CA°, where the TRF would autoignite much earlier in the cycle. The 5-C also continues to provide an excellent representation of the gasolines knocking behaviour in terms of KI, which is highly similar for the two fuels through the spark timing regime investigated. Mean KIs for both fuels increase as the spark timing is advanced from TDC, as does the standard deviation of KIs.

This is due to both the intrinsic difficulty in the analysis of the amplitude of highly transient pressure waves, caused by autoignition of the end gas, and the increasing severity of these pressure waves with earlier autoignition[3]. For severely knocking cases, a high degree of variability in KIs is expected as autoignition of the end gas can occur at spatially random points, the location of which influences the measured knocking pressure amplitude[14,59].

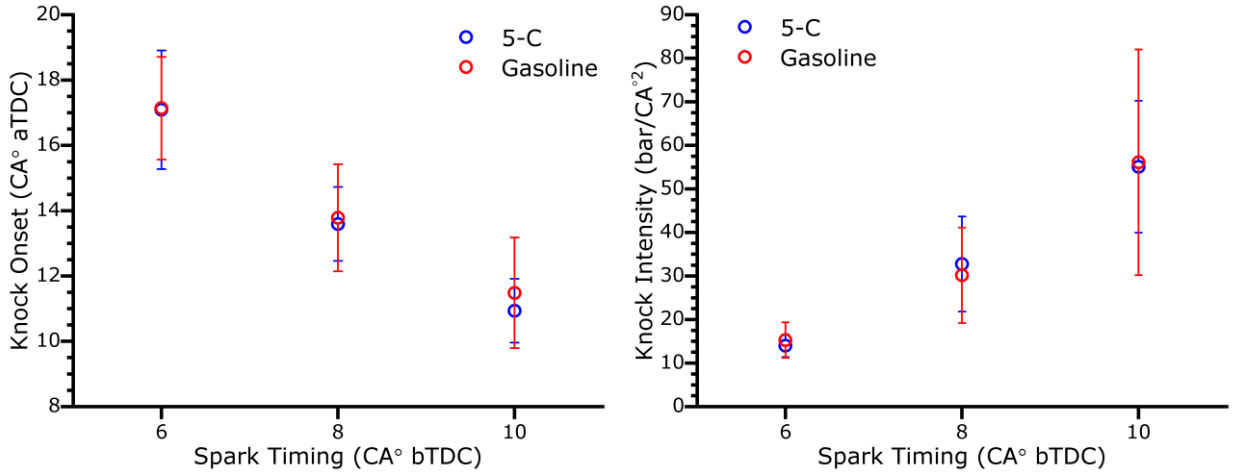

Figure 10. Mean KNs (left) and intensities (right) for 5-C and gasoline fuels, at all spark timings which displayed knocking cases. Error bars represent the standard deviation of values for each condition.

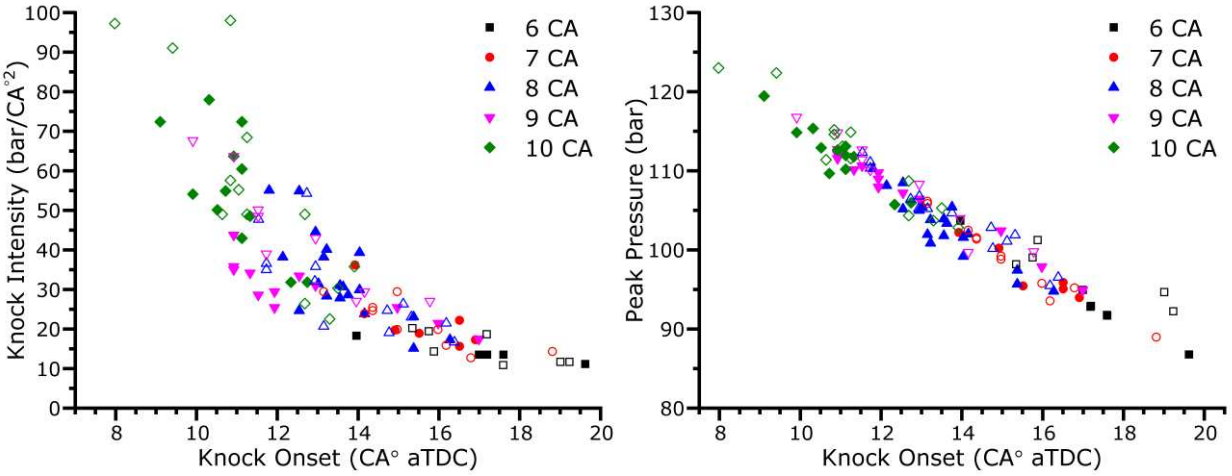

Figure 11. The relationship between KN and knock intensity (left), and peak pressure (right), for each firing cycle of the 5-C and gasoline fuels. Filled symbols represent 5-C data. Empty symbols represent gasoline data.

The relationship between KI and KN can be seen in figure 11 for each knocking cycle of the 5-C and gasoline fuels. Also shown in this figure is the relationship between peak pressure and KN for the same set of knocking cycles. Both the knocking intensity and peak pressures increase with spark advancement further from TDC and with decreasing KNs, for both the gasoline and 5-C. Therefore, as the occurrence of autoignition of the end gas moves earlier (towards TDC), the piston is closer to TDC and autoignition will occur under higher pressure conditions. While the relationship between knock intensity and onset, at a given spark timing appears to be linear, as seen in previous studies[3,35,36], the overall trend (totalling all spark timings for both gasoline and 5-C) is clearly non-linear, with the knock intensity increasing by greater amounts as the KN decreases and spark timing is advanced. The range of KNs, peak pressures and knock intensities is generally consistent between the surrogate and gasoline, however, at 10 CA° spark advance bTDC the gasoline displays a larger range of values at both the range top and bottom, but still produces mean values similar to those of 5-C. This is representative of the larger degrees of error seen for gasoline in figure 10 at this spark timings, as well as the larger cyclic variability observed for the gasoline in figure 9 and table 6. Overall, the 5-C provides an excellent representation of the reference gasoline under both normal and knocking combustion, accurately reproducing KNs, knock intensities and mean firing cycle behaviour. This supports similar conclusions on the surrogate's proficiency made on the basis of RCM IDT measurements[47].

3.4 The Influence of Iso-butanol on Engine Knock

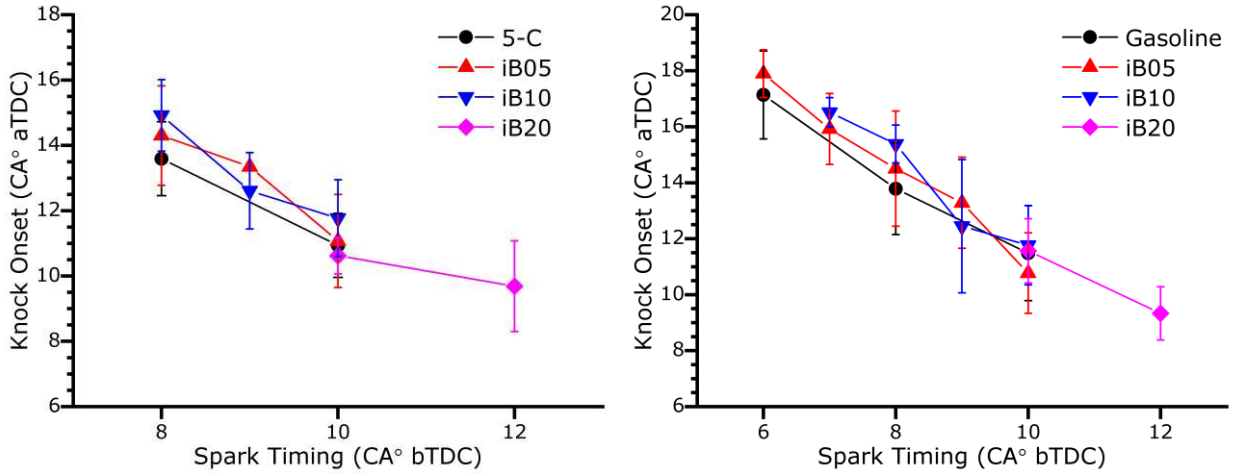

Figure 12. Mean KNs for iso-butanol blends with 5-C (left) and gasoline (right) fuels, at all spark timings which displayed knocking cases. Error bars represent the standard deviation of values for each condition.

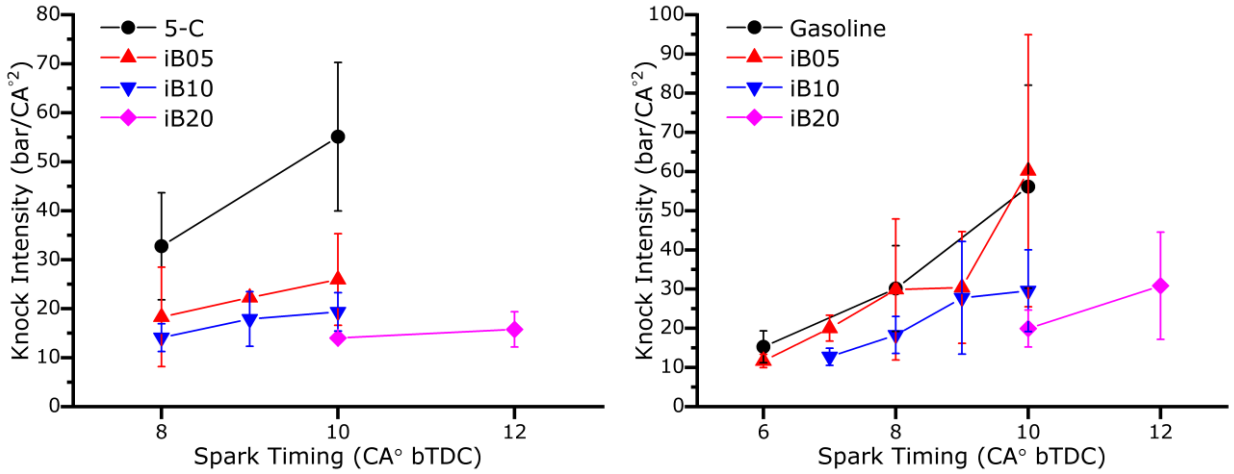

Figure 13. Mean knock intensities for iso-butanol blends with 5-C (left) and gasoline (right) fuels, at all spark timings which displayed knocking cases. Error bars represent the standard deviation of values for each condition.

The influence of iso-butanol addition on KN and KI can be seen in figures 12 and 13, respectively. Blends of 30-70% iso-butanol (iB30-iB70) are not present in these figures, as they did not produce any knocking cases at the investigated spark timings before the maximum safe

peak pressure of 120 bar was achieved. The high degree of knock resistance exhibited by these blends would allow an engine to operate at higher pressures, increasing engine efficiency. For small concentrations of iso-butanol (namely iB05 and iB10), knocking cases were observed at spark timings as low as 6 and 7 CA° bTDC for gasoline blends. However, knocking cases were not observed at the same spark advance timings in the case of 5-C blends. This is consistent with RCM results[47], which displayed slightly longer IDTs for the 5-C iB10, at a compressed temperature of ~770 K, correlating well with the unburnt gas temperatures predicted by engine modelling. In an engine, autoignition of the unburnt gas (knock) will occur when the end gas is unable to resist autoigniting before it is consumed by the advancing spark-initiated flame front, which subjects the unburnt gas to intense compression and heating. Knock is less likely to occur when the RCM measured IDT is longer. Small changes in IDT can manifest as significant changes in the autoignitive response of the unburned gas within an SI engine: an IDT difference of a millisecond in the RCM will translate to several crank angle degrees within the engine (in the case of this study, 1 ms = 4.5 CA°). In general, increasing the iso-butanol concentration causes an increase in the fuels knock resistance. However, non-linear behaviour is apparent at the lower blending ratios (iB05 and iB10). Similar non-linear behaviour was observed in normal combustion mean cycles, as well as RCM IDT measurements[47]. At spark timings up to 8 CA° bTDC, iB05 displays a greater resistance to knock than the neat fuels, with iB10 displaying a further increase. At a spark timing of 9 CA° bTDC, the KNs of the iB05 and iB10 fuels crossover, with iB05 now displaying the greatest knock resistance of the two blends. The same reactivity cross-over behaviour can be seen in gasoline and iso-butanol blends at the same spark timings. RCM measurements of IDT[47] also reflected this crossover behaviour between iB05 and iB10, at compressed temperatures of ~800-830 K..

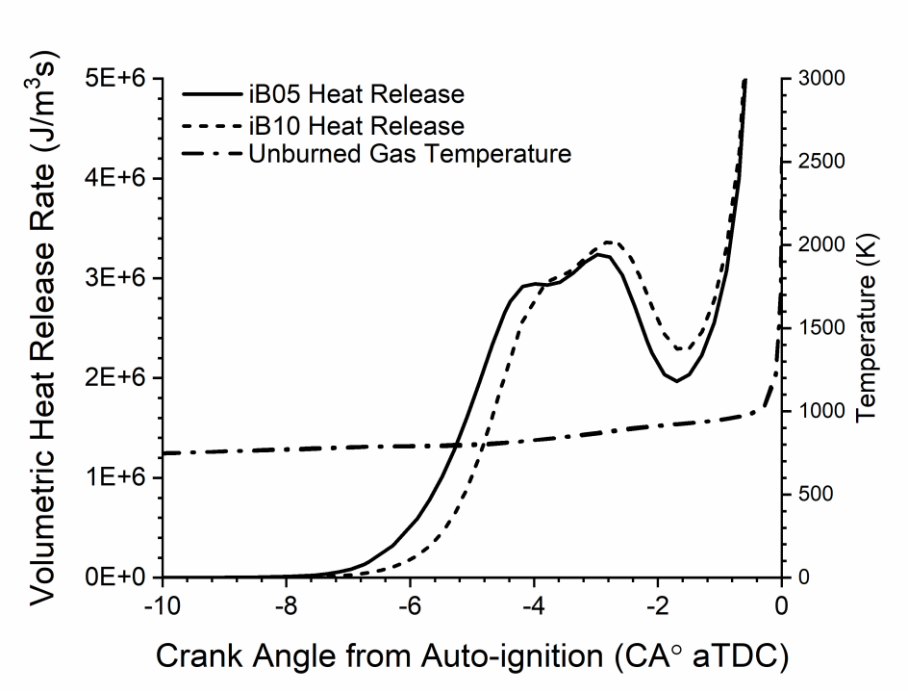

Figure 14. Engine modelling predictions of unburnt gas temperatures and volumetric heat release rates for 5-C blends of iB05 and iB10, at a spark advance timing of 9 CA° bTDC.

In the engine, this cross-over behaviour can be attributed to the suppression of the negative temperature coefficient (NTC) behaviour by iso-butanol addition, even in small quantities. Fuels which exhibit NTC behaviour show an increase in auto-ignitive resistance in this region, with increasing temperature. Zero-dimensional multi-zone engine modelling predicts unburnt gas temperatures for the iB05 and iB10 blends of approximately 790 K prior to the development of any significant LTHR, as shown in figure 14. This temperature falls within the NTC region for the iB05 fuel, as shown in previous RCM work[47], indicating that an increase in IDT and knock resistance is to be expected. However, due to suppression of NTC in the iB10 blends, no such increase in knock resistance is seen in this temperature region, causing IDTs and KNs to crossover with those of the iB05 blend. Local OH sensitivity analysis, for a zero-dimensional homogeneous batch reactor (designed to model autoignition within an RCM), has previously

shown the importance of iso-butanol chemistry in suppressing LTHR and NTC behaviour within this temperature region[47]. By applying brute-force sensitivity analysis to the LUPOE model, the sensitivity of KN to changes in reaction rate pre-exponential A-factors can be determined, and similar conclusions can be made. In this analysis, each reaction rate A-factor is varied independently and the impact of this change on the computed KN is used to determine sensitivity coefficients, such that $S_c=\log(KN_2/KN_{0.5})/\log(2/0.5)$, where KN_2 and $KN_{0.5}$ are the KNs corresponding to a change in the A-factor by factors of 2 and 0.5, respectively. Sensitivity coefficients for each reaction are then normalised by the maximum sensitivity at each spark advance timing, with a negative normalised sensitivity indicating a reduction in the crank angle location of KN and thus an increase in reactivity. Sensitivity analysis results for 5-C iB10 can be seen in figure 15, for spark advance timings of 8, 9 and 10 CA° bTDC. Here, the hydrogen abstraction from the primary iso-butanol (iC_4H_8OH) site by an OH radical is shown to be a dominant reaction, particularly at 10 CA° spark advance, where it is the most sensitive reaction, despite iso-butanol only contributing 10% of the blend's volume. This reaction is highly positively sensitive, indicating that an increase in this reaction rate produces a decrease in reactivity. The primary hydroxybutyl radical (iC_4H_8OH-1) produced may undergo further hydrogen abstraction to produce a relatively unreactive aldehyde and a HO_2 radical. These reactions provide an example of iso-butanol's behaviour as a radical scavenger during autoignition, consuming highly reactive OH radicals to form less reactive HO_2 radicals and aldehydes. This behaviour is important in generating the octane boosting qualities of iso-butanol but limits the generation of NTC behaviour[6,47]. Alternatively, the first oxygen addition to iC_4H_8OH-1 is shown to be negatively sensitive throughout the spark advance regime, as this opens a pathway to further low temperature oxidation. Similarly, hydrogen abstraction from iso-

butanol to form the tertiary hydroxybutyl radical (iC_4H_8OH-3) is also negatively sensitive, due to its higher propensity for low temperature chain branching when compared to the primary radical. This sensitivity increases as unburned gas temperatures increase, as the system more easily overcomes the higher bond dissociation energy (when compared to primary and secondary sites) at the tertiary site[73]. The same influence of iso-butanol can be seen in local OH sensitivity analysis of RCM simulations for 5-C and iso-butanol blends[47], providing further evidence for this behaviour and indicating the utility of fundamental experiments and less computationally expensive analysis in the prediction of phenomena in more complex systems (such as the LUPOE and associated engine modelling). Local OH sensitivity analysis results for RCM simulations are given in Supplementary Materials, for blends of iB10 and iB05 (supplementary figures S1 and S2, respectively), whereas analysis for 5-C can be found in the literature[47].

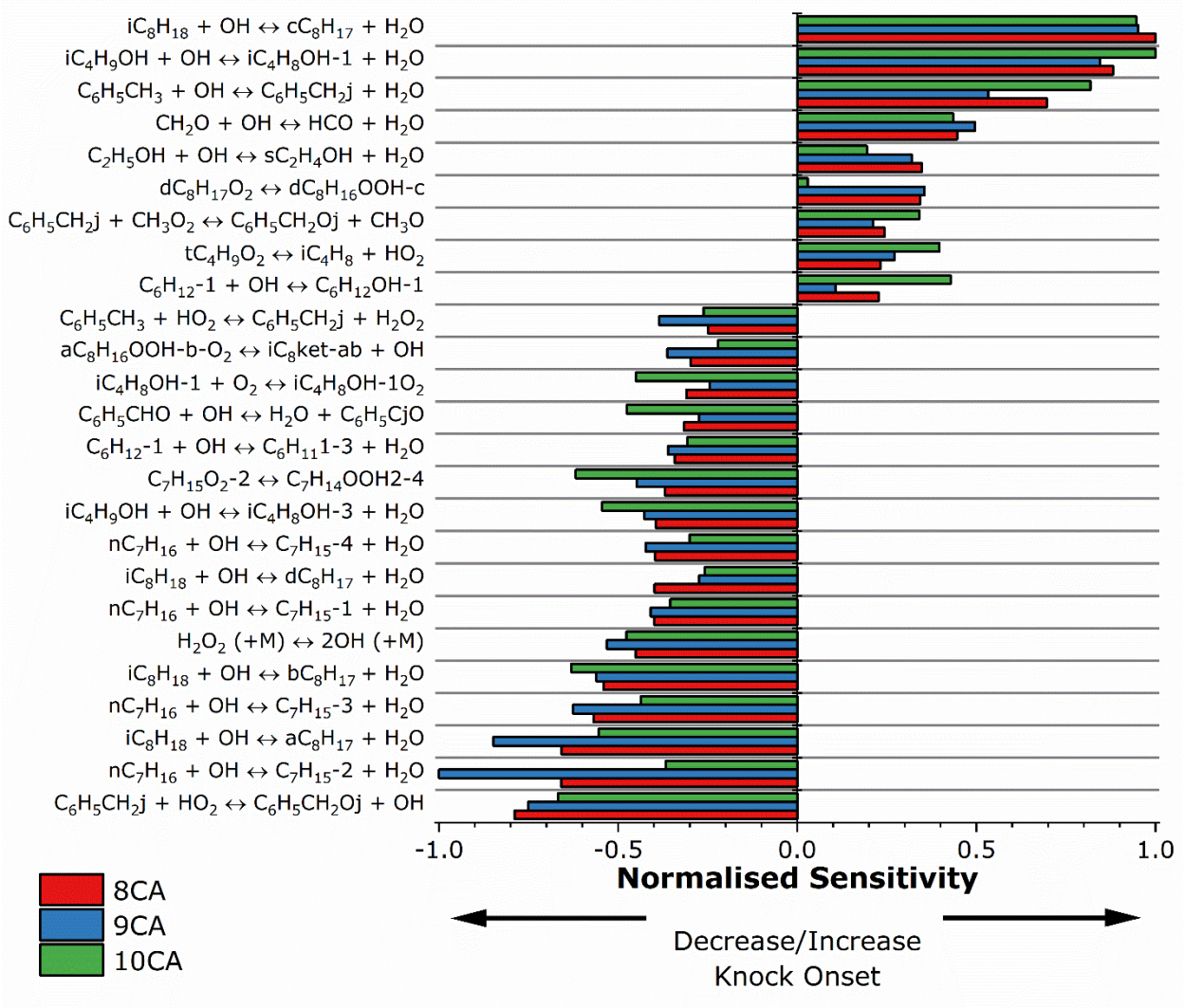

Figure 15. Normalised brute-force sensitivity analysis of KN modelling, results for iB10 at spark advance timings of 8, 9 and 10 CA° bTDC.

Sensitivity results for 5-C iB05, as shown in figure 16, do not exhibit the same degree of dominance by iso-butanol fuel reactions as seen for iB10. However, the primary hydrogen abstraction of iso-butanol to form iC_4H_8OH-1 does still appear to be highly positively sensitive, particularly considering the small volumetric fraction of iso-butanol in the fuel mixture. In the case of iB05, the scavenging of reactive OH radicals from the radical pool by iso-butanol may supress the NTC response, delaying it until increased temperatures facilitate a growing radical

pool. This leads to the delayed NTC witnessed in IDT measurements[47] (relative to 5-C) and therefore, the cross-over witnessed between iB05 and iB10 IDTs and KNs. Brute-force sensitivity analysis of the iB05 is otherwise dominated the fuel reactions of the 5-C components (toluene, iso-octane, n-heptane, ethanol, and 1-hexene), particularly the corresponding hydrogen abstractions by OH radicals. Throughout the investigated spark advance timing regime, reactivity is promoted by abstraction from the primary and secondary iso-octane sites, which may initiate chain branching further down the respective low temperature oxidation pathways. On the other hand, abstraction from the tertiary iso-octane site lacks a low temperature chain branching pathway, ultimately resulting in the formation of relatively unreactive olefin species from the initial iso-octane and OH radical[112]. Hydrogen abstractions from n-heptane display a highly negative sensitivity throughout the low temperature to NTC region, owing to the fuel's importance in the driving of first-stage ignition (cool flame). This is similar to the behaviour shown in sensitivity analysis of the 5-C, as shown in figure 17.

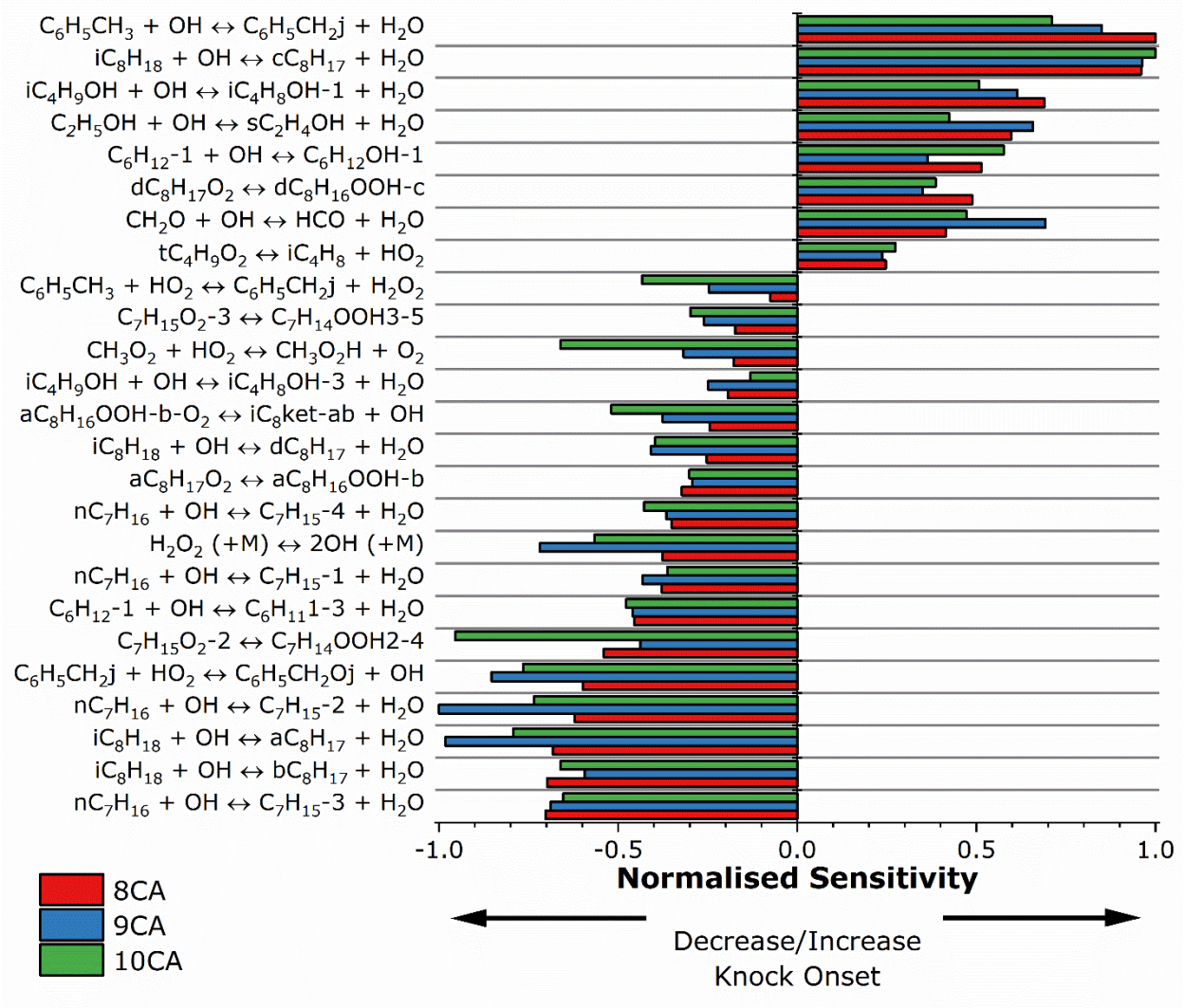

Figure 16. Normalised brute-force sensitivity analysis of KN modelling, results for iB05 at spark advance timings of 8, 9 and 10 CA° bTDC.

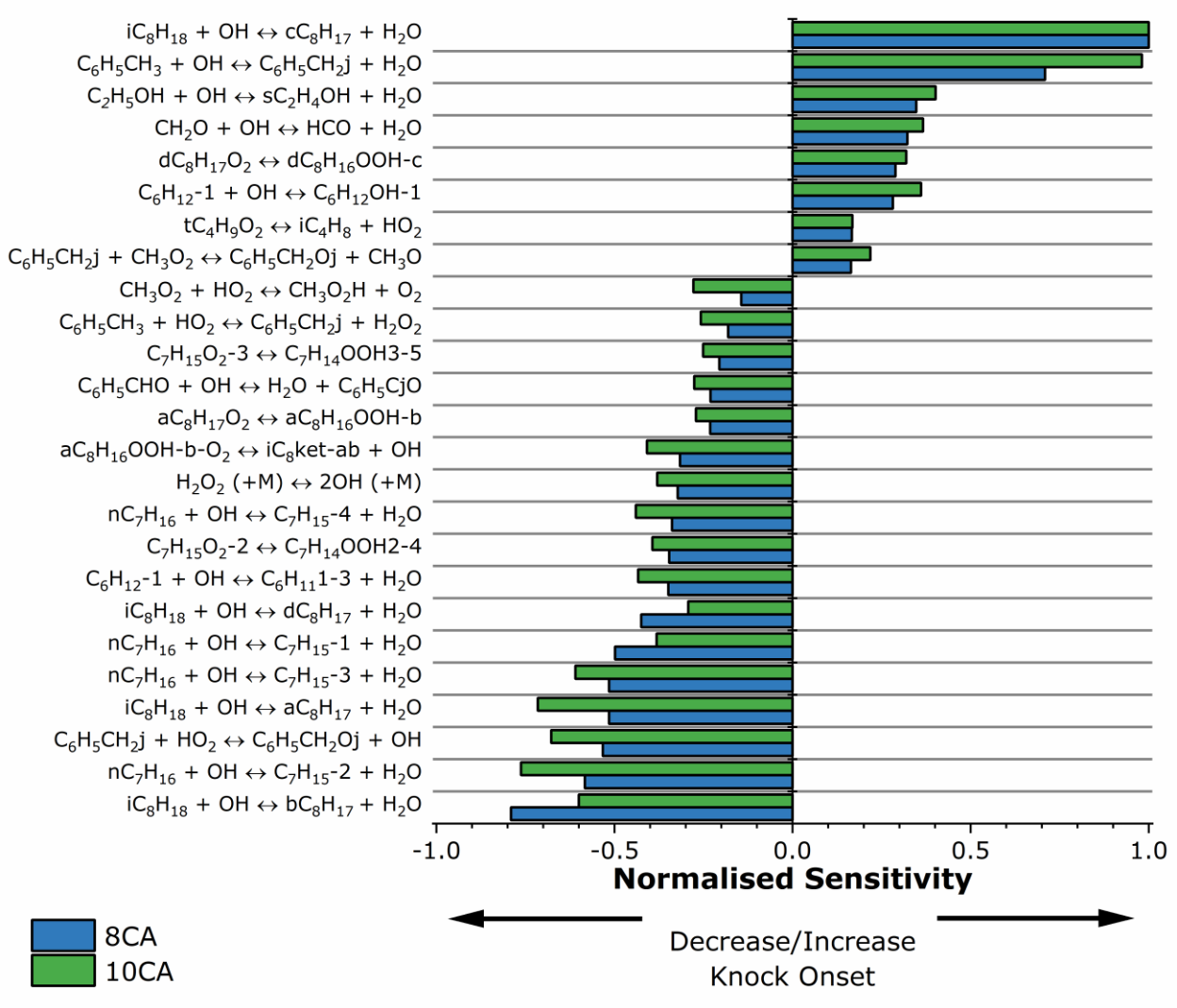

Figure 17. Normalised brute-force sensitivity analysis of KN modelling, results for 5-C at spark advance timings of 8 and 10 CA° bTDC.

Table 7. Cyclic variability for the knocking combustion of iso-butanol blends with 5-C and gasoline fuels, at a spark timing condition of 10 CA° bTDC, as represented by the CoV of peak pressure and the crank angle location of the peak pressure.

Base Fuel	**Iso-Butanol Content** (vol%)	**CoV$_{Pmax}$** (%)	**CoV$_{CA}$** (%)
Gasoline	**5**	**7.1**	**15**

	10	**5.3**	**11.6**
	20	**4.8**	**9.9**
5-C	**5**	**8.8**	**14**
	10	**4.9**	**10.1**
	20	**4.1**	**7.1**

An increase in the iso-butanol fraction of the blends generally produces a decrease in the observed KI. This is likely due to the suppression of LTHR by iso-butanol, which has been observed in heat release analysis of RCM experiments, wherein blends as low as 5% iso-butanol showed a large degree of heat release suppression in the LTHR region, reducing peak HRRs by approximately half at a compressed temperature of 710 K [47]. A significant reduction in the intensity of LTHR can also be seen in the engine modelling, as seen in figure 18, which shows the intensity of volumetric heat release for LTHR for knocking conditions of 5-C, iB05 and iB10 at a spark timing of 10 CA° bTDC, compared with the suppression of LTHR within the RCM, at the corresponding end gas temperature**.** This immediate and significant reduction in the magnitude of LTHR for both SI engine modelling and RCM corresponds with the appearance of iso-butanol hydrogen abstractions as highly sensitive reactions at relatively small iso-butanol concentrations, further highlighting the impacts of iso-butanol's radical scavenging behaviour on the suppression of typical alkane low temperature oxidation and NTC behaviour.

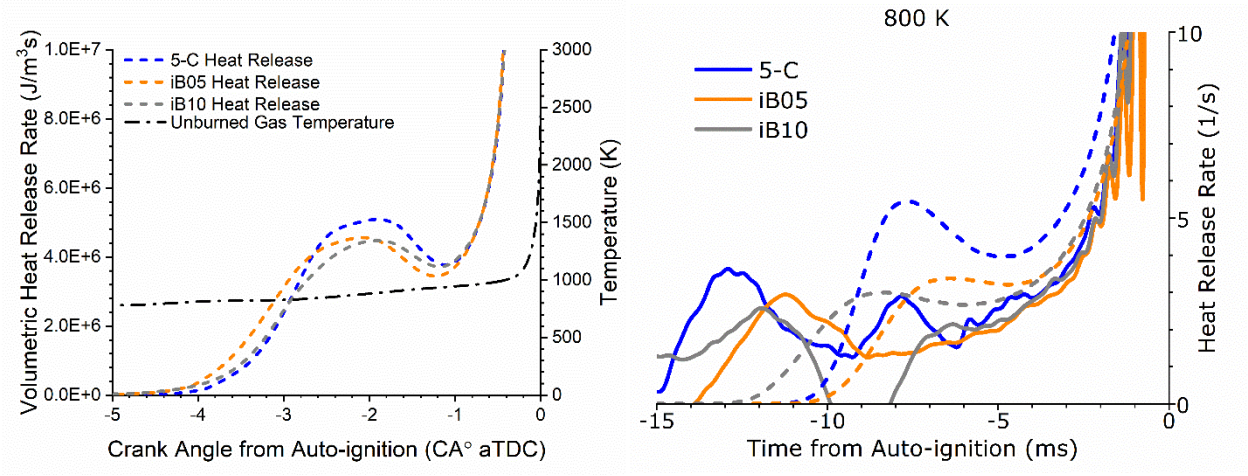

Figure 18. A comparison of LTHR as determined via engine modelling, RCM experimental analysis and RCM modelling, at the corresponding end gas temperature. (Left) shows the volumetric heat release rates for blends of 5-C, iB05 and iB10 at a spark timing of 10 CA° bTDC. (Right) shows LTHR behaviour as calculated from RCM and variable volume simulation data, at a compressed temperature of 800 K. Solid lines = RCM analysis. Dashed lines = simulation analysis. P_c=20 bar, Φ=1.

LTHR in SI engines can cause the enhancement of knock by increasing the intensity of second stage ignition[45]. It has been shown in the literature that suppression of LTHR through the application of fuel blending and additives can alter the knocking propensity of the fuel[113]. Blends of the 5-C with iso-butanol tend to produce lower KIs than the corresponding gasoline blends at the same conditions. A similar behaviour has been shown in the literature for blends of 20% n-butanol with the same reference gasoline and a TRF surrogate, wherein knock intensities for the n-butanol/TRF were considerably lower than the corresponding gasoline blend[3,35,36]. Gasoline/iso-butanol blends also tend to display a larger standard deviation of KIs throughout all conditions and blending ratios, as well as a higher degree of cyclic variability (as shown in table 7). Table 7 shows that increasing the iso-butanol fraction of gasoline also produces a decrease in

cyclic variability, which has positive implications for the use of such fuels under optimised SI engine conditions. While the 5-C blends also produce the same trend, the representation of the degree of cyclic variability exhibited by gasoline blends requires improvement. Cyclic variability is an important property which will need to be accounted for if computational models are to accurately predict the behaviour of gasoline blends.

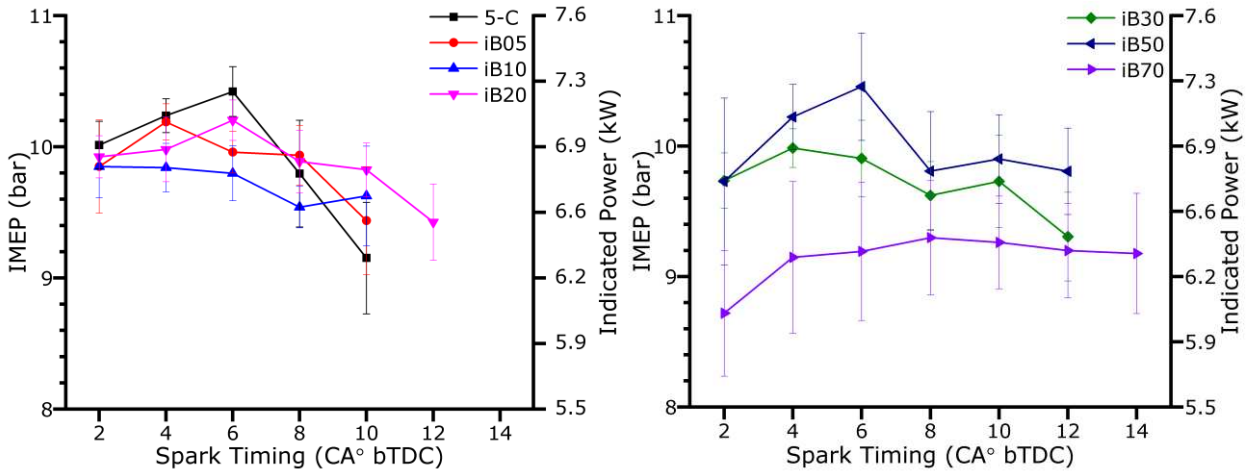

Figure 19. Mean IMEP values for 5-C/iso-butanol blends at each spark timing condition. Error bars represent the standard deviation of IMEP values in each case.

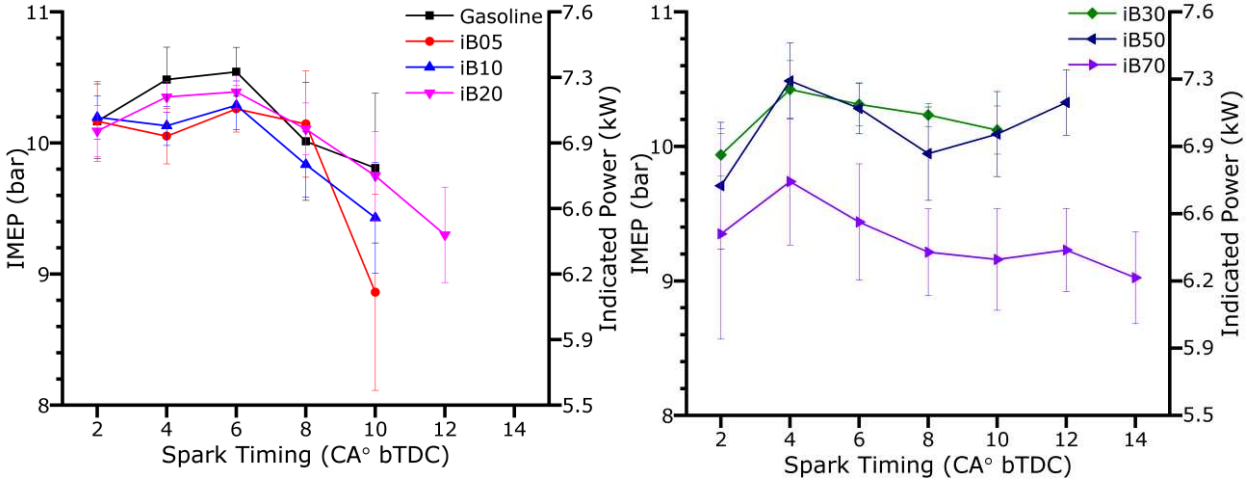

Figure 20. Mean IMEP values for gasoline/iso-butanol blends at each spark timing condition. Error bars represent the standard deviation of IMEP values in each case.

The influence of iso-butanol blending on the mean IMEP at various spark advance timings can be seen in figure 19 (for blends of 5-C and iso-butanol) and figure 20 (for blends of gasoline and iso-butanol). At spark timings of 2 to 6 CA° bTDC, blends of iB05 and iB10 produce mean IMEP values which are lower than those exhibited by the corresponding 5-C and gasoline blends. As the blending ratio is increased to iB20, the IMEP observably increases with spark advancement up to a timing of 6 CA° bTDC, for both 5-C and gasoline blends, but does not produce a mean IMEP larger than those displayed by the neat fuels. As spark timing is advanced further, the mean IMEPs of 5-C and gasoline reduce significantly. Due to this, at a spark advance timing of 8 CA°, a cross-over can be observed whereby the IMEPs of iB05 and iB20 are larger than the IMEP values of 5-C and gasoline. This is due to the increased knock resistance of these fuel blends, which allows for combustion to occur later in the engine cycle, minimising the work done by the combustion of the gas on the piston during compression. A marginal increase in IMEP has also been observed in the literature for blends of 20% iso-butanol with gasoline[22], which would lead to an increase in engine power as well as the increased knock resistance of the fuel. At a spark timing of 10 CA° bTDC, significant differences can be observed between 5-C and gasoline blended fuels. Gasoline iB05 produces a much lower value for IMEP than that seen for 5-C iB05, which may be due to the prevalence of high intensity knock at this condition. Also, in general IMEP values are lower for 5-C blends than gasoline blends, particularly at normal combustion conditions (spark timings < 6 CA° bTDC). The increased knock resistance of iB20 blends produces IMEP values equivalent to or larger than the corresponding neat fuel value at a spark timing of 10 CA° bTDC. For 5-C, the blend of 30% iso-butanol (iB30) produces similar IMEPs to iB20 at spark timings of 2 and 4 CA° but appears to show lower mean IMEP values at longer spark advance timings. A reduction in brake power for blends of 30% iso-butanol with

gasoline has also been observed in the literature[18]. Gasoline blends also display a marginal reduction in IMEP for the iB30, when compared to gasoline, at spark advance timings of 4 and 6 CA° bTDC. Otherwise, the gasoline iB30 produces IMEPs consistently larger than the neat gasoline, whereas 5-C iB30 only displays larger mean IMEPs at spark timings of 10 and 12 CA° bTDC. At these timings, the enhanced knock resistance of the iB30 delays the development of high combustion pressures until later in the piston cycle.

For blends of 30-70% iso-butanol, IMEPs at a spark advance timing of 2 CA° bTDC are considerably lower than those for the neat fuels and blends of low iso-butanol concentration, which is indicative of the much lower peak pressures observed at this blending ratio, as seen in figure 6. At spark timings of 4 and 6 CA° bTDC, iB50 displays IMEPs larger than or approximately equivalent to those displayed by the neat fuels. As spark timing is advanced further, IMEPs for iB50 are considerably larger than those displayed by the neat fuels due to the influence of knock and the high knocking resistance of the iB50 blends. Blends of iB50 were investigated at spark advance timings of up to 14 CA° bTDC (until the maximum safe peak pressure was achieved) and no knocking cases were observed, showing that the blend is capable of operating at much earlier spark advance timings than the neat fuels and lower concentration iso-butanol blends. The capability of a fuel to operate effectively at spark timings far from TDC is important for SI engine performance, as if the knock limited spark advance is closer to TDC than the maximum brake torque timing, engine performance is limited by knock. Therefore, a fuel with a high degree of knock resistance allows for the further advancement of spark timing towards the maximum brake torque timing. However, the high degree of cyclic variability displayed by blends which contain a large volume of iso-butanol must also be considered, as this makes the SI engine difficult to optimise and may impact performance and driveability.

4 Conclusions

In this study, the normal and knocking combustion behaviour of gasoline, a five-component surrogate (5-C) and their respective blends with iso-butanol was studied experimentally within the LUPOE-2D to determine the influence of iso-butanol of SI engine performance and the ability of a surrogate to replicate the combustion behaviour of gasoline. This work showed that 5-C produced a good representation of the reference gasoline's mean pressure development during normal SI combustion, particularly when compared to a three component TRF surrogate investigated in the literature[3,32,35,36]. The mean peak pressure, crank angle location of the mean peak pressure and the evolution of the pressure gradient during combustion were all highly similar between the surrogate and reference gasoline. However, cyclic variability was somewhat larger for 5-C at normal combustion conditions. In the presence of engine knock, the representation of the reference gasoline by the 5-C was excellent, with 5-C accurately representing mean KNs and KIs throughout the investigated regime. When compared with RCM IDT measurements presented in the literature[47], it would appear that a good representation of gasolines knocking behaviour in the engine, correlates with a good representation of homogeneous IDTs in the RCM. Spark advance timings of 6-10 CA° bTDC correlate with end gas temperatures during the onset of first stage heat release of ~750-830 K, according to unburnt gas temperatures predicted by the engine model. Within this temperature range, IDTs for the gasoline and 5-C are very closely matched, which coincides with an excellent representation of knocking behaviour within the engine. At a compressed temperature of 870 K, gasoline displayed slightly longer IDTs than 5-C, whereas from ~770-830 K the two fuels produced IDTs within uncertainty limits of each other. This lower reactivity for gasoline at the higher temperature end of the scale is also present in KN measurements. These trends highlight the

usefulness of RCMs a tool for assessing the capabilities of surrogates for use in an SI engine, at least under the conditions investigated in this study.

Generally, iso-butanol blending produced a greater degree of knock resistance with increasing iso-butanol concentration. Blends of larger than 30% iso-butanol content by volume produced no knocking cases at all spark advance timings that could be safely investigated. Blending of iso-butanol with both 5-C and gasoline displayed a non-linear behaviour at a spark timing of 9 CA° bTDC, wherein iB05 displayed a later KN than the iB10 blends. This correlated well with previous RCM measurements of IDT for iB05 and iB10 blends[47], at compressed temperatures of ~790K, which aligns with predicted end gas temperatures at a spark timing of 9 CA° bTDC. This unburnt gas temperature coincides with an increase in IDTs for the iB05 due to the presence of clear NTC behaviour, which is heavily supressed in the iB10 fuel due to the role of iso-butanol as a strong radical sink, as identified by brute-force sensitivity analysis of KNs predicted by zero-dimensional engine modelling. Increasing iso-butanol concentration also produced a decrease in the apparent KIs. This is indicative of iso-butanol's role in supressing LTHR, as shown through the heat release analysis of RCM experiments at conditions appropriate for unburnt gas temperatures, as well as the analysis of zero-dimensional engine modelling. Both of these methods highlighted the suppression of LTHR by even small additions of iso-butanol. Blends with a greater knock resistance were shown to produce larger IMEP values at spark advance timings longer than 6 CA° bTDC. The iB50 blend displayed IMEP values close to those for the neat fuels under normal combustion, at spark advance timings of up to 14 CA° bTDC. At this condition, all cycles were free of knock, and the maximum safe working pressure of 120 bar was achieved. The ability to advance the spark timing further from TDC towards the maximum brake torque timing, with minimal impacts on the work done per cycle, may lead to

improvements in SI engine performance. At short spark advance timings, the iB50 blend produced a large increase in cyclic variability when compared to gasoline and blends of lower iso-butanol concentration. However, as spark timing is advanced further from TDC, this variability decreases, meaning that this fuel may be viable if operated at such spark timings. Operating at large spark advance timings would also need to occur to maximise the benefit of the fuel's large degree of knock resistance and reasonable engine power at these conditions.

From the trends in this study, due to the influence of iso-butanol blending on the combustion behaviour of gasoline, 20-50% iso-butanol by volume appears to produce a range of fuels suitable for use in pressure boosted SI engines. The widescale use of any blend in this range would impact significantly on the requirements of the RED II, which requires a minimum of 14% renewable fuels for all road and rail transport, with at least 3.5% coming from advanced biofuels, by 2030[5]. However, meeting the production needs for large quantities of iso-butanol would be difficult currently, as iso-butanol yields are limited due to both process and economic constraints[114,115]. Therefore, it is recommended that blends of 20-30% be implemented as these provide many of the benefits of higher iso-butanol concentrations but with lower biofuel quantities required. Future work on the influence of iso-butanol blending with gasoline for use is SI engines should focus on the investigation of iso-butanol's impact on flame characteristics, in both fundamental systems (bomb calorimeter) and optical SI engines, particularly as the burning rate and charge cooling influence of iso-butanol are proposed to impact on combustion performance within the engine. Flame imaging and laminar burning velocity measurements for such blends also appear to be absent in the literature and would be valuable, with laminar burning velocities serving as important kinetic modelling validation targets. Furthermore, for consideration for real-world applications, the impact of blending on emissions requires further

investigation. While some studies have been conducted into the emissions characteristics of iso-butanol/gasoline blends, these tend to focus on a narrow range of blends and engine operating parameters [21,22,116,117]. These laboratory emissions tests also do not provide a full picture of the fuel's emission behaviour during real driving conditions. To develop an understanding of the impact of iso-butanol on practical emissions, there is a need to investigate each blend over a wide range of conditions relevant to the conditions observed during real world vehicle use [118]. Therefore, future emissions testing of iso-butanol/gasoline blended fuels should evaluate the impact of blending on real driving emissions, through the use of a research vehicle and real driving emissions (RDE) tests [118], as well as laboratory based emissions test cycles.

5 Author Information

Corresponding Author

*E-mail: c.michelbach@leeds.ac.uk

Funding Sources

This research is supported by the EPSRC training grant: EP/L014912/1, regulated by the University of Leeds Centre for Doctoral Training in Bioenergy.

6 Supporting Information

Supplementary materials are provided which show normalised local OH sensitivity analysis results for zero-dimensional homogeneous RCM simulations, for blends of 5-C iB10 and 5-C iB05, at SI engine relevant conditions.

7 Acknowledgements

Grateful thanks are offered to the Thermofluids laboratory technical support: Mark Batchelor, Samuel Flint and Peter Grieve for their assistance in the operation and maintenance of the LUPOE-2D engine facility. Thanks, are also given to Derek Bradley and Malcolm Lawes for their valuable input during the project. Specific acknowledgements must be extended to Wankang “Peter” Zhang and Junior “James” Achumu for sacrificing their time to provide LUPOE-2D training and support during the completion of this study. Also, thanks go to Roger Cracknell and Shell Global Solutions for the provision of the gasoline fuel.

8 References

(1) AlRamadan, A. S.; Badra, J.; Javed, T.; Al-Abbad, M.; Bokhumseen, N.; Gaillard, P.; Babiker, H.; Farooq, A.; Sarathy, S. M. Mixed Butanols Addition to Gasoline Surrogates: Shock Tube Ignition Delay Time Measurements and Chemical Kinetic Modeling. *Combust. Flame* **2015**, *162* (10), 3971–3979. https://doi.org/10.1016/j.combustflame.2015.07.035.

(2) Agbro, E.; Tomlin, A. S.; Lawes, M.; Park, S.; Sarathy, S. M. The Influence of n -Butanol Blending on the Ignition Delay Times of Gasoline and Its Surrogate at High Pressures. *Fuel* **2017**, *187*, 211–219. https://doi.org/10.1016/j.fuel.2016.09.052.

(3) Agbro, E.; Zhang, W.; Tomlin, A. S.; Burluka, A. Experimental Study on the Influence of *n* -Butanol Blending on the Combustion, Autoignition, and Knock Properties of Gasoline and Its Surrogate in a Spark-Ignition Engine. *Energy Fuels* **2018**, *32* (10), 10052–10064. https://doi.org/10.1021/acs.energyfuels.8b00713.

(4) Gorbatenko, I.; Tomlin, A. S.; Lawes, M.; Cracknell, R. F. Experimental and Modelling Study of the Impacts of N-Butanol Blending on the Auto-Ignition Behaviour of Gasoline and Its Surrogate at Low Temperatures. *Proc. Combust. Inst.* **2019**, *37* (1), 501–509. https://doi.org/10.1016/j.proci.2018.05.089.

(5) European Commission. DIRECTIVE (EU) 2018/ 2001 OF THE EUROPEAN PARLIAMENT AND OF THE COUNCIL - of 11 December 2018 - on the Promotion of the Use of Energy from Renewable Sources. *Off. J. Eur. Union* **2018**, 128.

(6) Sarathy, S. M.; Oßwald, P.; Hansen, N.; Kohse-Höinghaus, K. Alcohol Combustion Chemistry. *Prog. Energy Combust. Sci.* **2014**, *44*, 40–102. https://doi.org/10.1016/j.pecs.2014.04.003.

(7) Szwaja, S.; Naber, J. D. Combustion of N-Butanol in a Spark-Ignition IC Engine. *Fuel* **2010**, *89* (7), 1573–1582. https://doi.org/10.1016/j.fuel.2009.08.043.

(8) Wallner, T.; Miers, S. A.; McConnell, S. A Comparison of Ethanol and Butanol as Oxygenates Using a Direct-Injection, Spark-Ignition (DISI) Engine; American Society of Mechanical Engineers Digital Collection, 2009; pp 129–139. https://doi.org/10.1115/ICES2008-1690.

(9) Szulczyk, K. Which Is a Better Transportation Fuel - Butanol or Ethanol? *Int. J. Energy Environ.* **2010**, *1*.

(10) Wigg, B. R. A Study on the Emissions of Butanol Using a Spark Ignition Engine and Their Reduction Using Electrostatically Assisted Injection, University of Illinois at Urbana-Champaign, 2011.

(11) Lapuerta, M.; García-Contreras, R.; Campos-Fernández, J.; Dorado, M. P. Stability, Lubricity, Viscosity, and Cold-Flow Properties of Alcohol−Diesel Blends. *Energy Fuels* **2010**, *24* (8), 4497–4502. https://doi.org/10.1021/ef100498u.

(12) Skevis, G. Liquid Biofuels: Bioalcohols, Biodiesel and Biogasoline and Algal Biofuels. In *Handbook of Combustion*; American Cancer Society, 2016; pp 1–43. https://doi.org/10.1002/9783527628148.hoc051.pub2.

(13) Weber, B. W.; Sung, C.-J. Comparative Autoignition Trends in Butanol Isomers at Elevated Pressure. *Energy Fuels* **2013**, *27* (3), 1688–1698. https://doi.org/10.1021/ef302195c.

(14) Konig, G.; Sheppard, C. G. W. End Gas Autoignition and Knock in a Spark Ignition Engine; 1990; p 902135. https://doi.org/10.4271/902135.

(15) Heywood, J. *Internal Combustion Engine Fundamentals*; McGraw-Hill Education, 1988.
(16) Wang, Z.; Liu, H.; Song, T.; Qi, Y.; He, X.; Shuai, S.; Wang, J. Relationship between Super-Knock and Pre-Ignition. *Int. J. Engine Res.* **2015**, *16* (2), 166–180. https://doi.org/10.1177/1468087414530388.
(17) Kalghatgi, G. T. Developments in Internal Combustion Engines and Implications for Combustion Science and Future Transport Fuels. *Proc. Combust. Inst.* **2015**, *35* (1), 101–115. https://doi.org/10.1016/j.proci.2014.10.002.
(18) Alasfour, F. N. Butanol—A Single-Cylinder Engine Study: Availability Analysis. *Appl. Therm. Eng.* **1997**, *17* (6), 537–549. https://doi.org/10.1016/S1359-4311(96)00069-5.
(19) Irimescu, A. Performance and Fuel Conversion Efficiency of a Spark Ignition Engine Fueled with Iso-Butanol. *Appl. Energy* **2012**, *96*, 477–483. https://doi.org/10.1016/j.apenergy.2012.03.012.
(20) Elfasakhany, A. Experimental Investigation on SI Engine Using Gasoline and a Hybrid Iso-Butanol/Gasoline Fuel. *Energy Convers. Manag.* **2015**, *95*, 398–405. https://doi.org/10.1016/j.enconman.2015.02.022.
(21) Li, Y.; Ning, Z.; Yan, J.; Lee, T. H.; Lee, C. F. Experimental Investigation on Combustion and Unregulated Emission Characteristics of Butanol-Isomer/Gasoline Blends. *J. Cent. South Univ.* **2019**, *26* (8), 2244–2258. https://doi.org/10.1007/s11771-019-4170-z.
(22) Anselmi, P.; Matrat, M.; Starck, L.; Duffour, F. Combustion Characteristics of Oxygenated Fuels Ethanol-and Butanol-Gasoline Fuel Blends, and Their Impact on Performance, Emissions and Soot Index; 2019; pp 2019-01–2307. https://doi.org/10.4271/2019-01-2307.
(23) Tomlin, A. S.; Turányi, T.; Pilling, M. J. Chapter 4 Mathematical Tools for the Construction, Investigation and Reduction of Combustion Mechanisms. In *Comprehensive Chemical Kinetics*; Pilling, M. J., Ed.; Low-Temperature Combustion and Autoignition; Elsevier, 1997; Vol. 35, pp 293–437. https://doi.org/10.1016/S0069-8040(97)80019-2.
(24) Griffiths, J. F.; Mohamed, C. Chapter 6 Experimental and Numerical Studies of Oxidation Chemistry and Spontaneous Ignition Phenomena. In *Comprehensive Chemical Kinetics*; Pilling, M. J., Ed.; Low-Temperature Combustion and Autoignition; Elsevier, 1997; Vol. 35, pp 545–660. https://doi.org/10.1016/S0069-8040(97)80021-0.
(25) Khan, A. F.; Burluka, A.; Neumeister, J.; OudeNijeweme, D.; Freeland, P.; Mitcalf, J. Combustion and Autoignition Modelling in a Turbocharged SI Engine. *SAE Int. J. Engines* **2016**, *9* (4), 2079–2090. https://doi.org/10.4271/2016-01-2234.
(26) Kukkadapu, G.; Kumar, K.; Sung, C.-J.; Mehl, M.; Pitz, W. J. Autoignition of Gasoline and Its Surrogates in a Rapid Compression Machine. *Proc. Combust. Inst.* **2013**, *34* (1), 345–352. https://doi.org/10.1016/j.proci.2012.06.135.
(27) Chung, J.; Lee, S.; An, H.; Song, S.; Chun, K. M. Rapid-Compression Machine Studies on Two-Stage Ignition Characteristics of Hydrocarbon Autoignition and an Investigation of New Gasoline Surrogates. *Energy* **2015**, *93*, 1505–1514. https://doi.org/10.1016/j.energy.2015.09.077.
(28) Lee, C.; Ahmed, A.; Nasir, E. F.; Badra, J.; Kalghatgi, G.; Sarathy, S. M.; Curran, H.; Farooq, A. Autoignition Characteristics of Oxygenated Gasolines. *Combust. Flame* **2017**, *186*, 114–128. https://doi.org/10.1016/j.combustflame.2017.07.034.
(29) Javed, T.; Lee, C.; AlAbbad, M.; Djebbi, K.; Beshir, M.; Badra, J.; Curran, H.; Farooq, A. Ignition Studies of N-Heptane/Iso-Octane/Toluene Blends. *Combust. Flame* **2016**, *171*, 223–233. https://doi.org/10.1016/j.combustflame.2016.06.008.

(30) Kang, D.; Fridlyand, A.; Goldsborough, S. S.; Wagnon, S. W.; Mehl, M.; Pitz, W. J.; McNenly, M. J. Auto-Ignition Study of FACE Gasoline and Its Surrogates at Advanced IC Engine Conditions. *Proc. Combust. Inst.* **2019**, *37* (4), 4699–4707. https://doi.org/10.1016/j.proci.2018.08.053.
(31) Sarathy, S. M.; Kukkadapu, G.; Mehl, M.; Javed, T.; Ahmed, A.; Naser, N.; Tekawade, A.; Kosiba, G.; AlAbbad, M.; Singh, E.; Park, S.; Rashidi, M. A.; Chung, S. H.; Roberts, W. L.; Oehlschlaeger, M. A.; Sung, C.-J.; Farooq, A. Compositional Effects on the Ignition of FACE Gasolines. *Combust. Flame* **2016**, *169*, 171–193. https://doi.org/10.1016/j.combustflame.2016.04.010.
(32) Pera, C.; Knop, V. Methodology to Define Gasoline Surrogates Dedicated to Auto-Ignition in Engines. *Fuel* **2012**, *96*, 59–69. https://doi.org/10.1016/j.fuel.2012.01.008.
(33) Khan, A. F.; Roberts, P. J.; Burluka, A. A. Modelling of Self-Ignition in Spark-Ignition Engine Using Reduced Chemical Kinetics for Gasoline Surrogates. *Fluids* **2019**, *4* (3), 157. https://doi.org/10.3390/fluids4030157.
(34) Ahmed, A.; Goteng, G.; Shankar, V. S. B.; Al-Qurashi, K.; Roberts, W. L.; Sarathy, S. M. A Computational Methodology for Formulating Gasoline Surrogate Fuels with Accurate Physical and Chemical Kinetic Properties. *Fuel* **2015**, *143*, 290–300. https://doi.org/10.1016/j.fuel.2014.11.022.
(35) Agbro, E. B. Experimental and Chemical Kinetic Modelling Study on the Combustion of Alternative Fuels in Fundamental Systems and Practical Engines. phd, University of Leeds, 2017.
(36) Zhang, W. Measurements of Flow and Combustion in a Strongly Charged Spark Ignition Engine. phd, University of Leeds, 2018.
(37) Hunwartzen, I. Modification of CFR Test Engine Unit to Determine Octane Numbers of Pure Alcohols and Gasoline-Alcohol Blends; 1982; p 820002. https://doi.org/10.4271/820002.
(38) Anderson, J. E.; Kramer, U.; Mueller, S. A.; Wallington, T. J. Octane Numbers of Ethanol− and Methanol−Gasoline Blends Estimated from Molar Concentrations. *Energy Fuels* **2010**, *24* (12), 6576–6585. https://doi.org/10.1021/ef101125c.
(39) Anderson, J. E.; Leone, T. G.; Shelby, M. H.; Wallington, T. J.; Bizub, J. J.; Foster, M.; Lynskey, M. G.; Polovina, D. Octane Numbers of Ethanol-Gasoline Blends: Measurements and Novel Estimation Method from Molar Composition; 2012; pp 2012-01–1274. https://doi.org/10.4271/2012-01-1274.
(40) Foong, T. M.; Morganti, K. J.; Brear, M. J.; da Silva, G.; Yang, Y.; Dryer, F. L. The Octane Numbers of Ethanol Blended with Gasoline and Its Surrogates. *Fuel* **2014**, *115*, 727–739. https://doi.org/10.1016/j.fuel.2013.07.105.
(41) AlRamadan, A. S.; Sarathy, S. M.; Khurshid, M.; Badra, J. A Blending Rule for Octane Numbers of PRFs and TPRFs with Ethanol. *Fuel* **2016**, *180*, 175–186. https://doi.org/10.1016/j.fuel.2016.04.032.
(42) Haas, F. M.; Chaos, M.; Dryer, F. L. Low and Intermediate Temperature Oxidation of Ethanol and Ethanol–PRF Blends: An Experimental and Modeling Study. *Combust. Flame* **2009**, *156* (12), 2346–2350. https://doi.org/10.1016/j.combustflame.2009.08.012.
(43) Karwat, D. M. A.; Wagnon, S. W.; Wooldridge, M. S.; Westbrook, C. K. On the Combustion Chemistry of N-Heptane and n-Butanol Blends. *J. Phys. Chem. A* **2012**, *116* (51), 12406–12421. https://doi.org/10.1021/jp309358h.

(44) Zhang, J.; Niu, S.; Zhang, Y.; Tang, C.; Jiang, X.; Hu, E.; Huang, Z. Experimental and Modeling Study of the Auto-Ignition of n-Heptane/n-Butanol Mixtures. *Combust. Flame* **2013**, *160* (1), 31–39. https://doi.org/10.1016/j.combustflame.2012.09.006.
(45) Agbro, E.; Tomlin, A. S.; Zhang, W.; Burluka, A.; Mauss, F.; Pasternak, M.; Alfazazi, A.; Sarathy, S. M. Chemical Kinetic Modeling Study on the Influence of *n* -Butanol Blending on the Combustion, Autoignition, and Knock Properties of Gasoline and Its Surrogate in a Spark-Ignition Engine. *Energy Fuels* **2018**, *32* (10), 10065–10077. https://doi.org/10.1021/acs.energyfuels.8b00962.
(46) Goldsborough, S. S.; Cheng, S.; Kang, D.; Saggese, C.; Wagnon, S. W.; Pitz, W. J. Effects of Isoalcohol Blending with Gasoline on Autoignition Behavior in a Rapid Compression Machine: Isopropanol and Isobutanol. *Proc. Combust. Inst.* **2021**, *38* (4), 5655–5664. https://doi.org/10.1016/j.proci.2020.08.027.
(47) Michelbach, C.; Tomlin, A. An Experimental and Kinetic Modeling Study of the Ignition Delay and Heat Release Characteristics of a Five Component Gasoline Surrogate and Its Blends with Iso-Butanol within a Rapid Compression Machine. *Int. J. Chem. Kinet.* **2021**, *53* (6), 787–808. https://doi.org/10.1002/kin.21483.
(48) Fan, Y.; Duan, Y.; Han, D.; Qiao, X.; Huang, Z. Influences of Isomeric Butanol Addition on Anti-Knock Tendency of Primary Reference Fuel and Toluene Primary Reference Fuel Gasoline Surrogates. *Int. J. Engine Res.* **2021**, *22* (1), 39–49. https://doi.org/10.1177/1468087419850704.
(49) Han, D.; Fan, Y.; Sun, Z.; Nour, M.; Li, X. Combustion and Emissions of Isomeric Butanol/Gasoline Surrogates Blends on an Optical GDI Engine. *Fuel* **2020**, *272*, 117690. https://doi.org/10.1016/j.fuel.2020.117690.
(50) Jesu Godwin, D.; Edwin Geo, V.; Thiyagarajan, S.; Leenus Jesu Martin, M.; Maiyalagan, T.; Saravanan, C. G.; Aloui, F. Effect of Hydroxyl (OH) Group Position in Alcohol on Performance, Emission and Combustion Characteristics of SI Engine. *Energy Convers. Manag.* **2019**, *189*, 195–201. https://doi.org/10.1016/j.enconman.2019.03.063.
(51) Burluka, A. A.; El-Dein Hussin, A. M. T. A.; Ling, Z.-Y.; Sheppard, C. G. W. Effects of Large-Scale Turbulence on Cyclic Variability in Spark-Ignition Engine. *Exp. Therm. Fluid Sci.* **2012**, *43*, 13–22. https://doi.org/10.1016/j.expthermflusci.2012.04.012.
(52) Ling, Z.; Burluka, A.; Azimov, U. Knock Properties of Oxygenated Blends in Strongly Charged and Variable Compression Ratio Engines; 2014; pp 2014-01–2608. https://doi.org/10.4271/2014-01-2608.
(53) Warnatz, J.; Maas, U.; Dibble, R. W. *Combustion: Physical and Chemical Fundamentals, Modeling and Simulation, Experiments, Pollutant Formation*, 4th ed.; Springer-Verlag: Berlin Heidelberg, 2006. https://doi.org/10.1007/978-3-540-45363-5.
(54) Hirooka, H.; Mori, S.; Shimizu, R. Effects of High Turbulence Flow on Knock Characteristics; 2004; pp 2004-01–0977. https://doi.org/10.4271/2004-01-0977.
(55) Mittal, V.; Revier, B. M.; Heywood, J. B. Phenomena That Determine Knock Onset in Spark-Ignition Engines; 2007; pp 2007-01–0007. https://doi.org/10.4271/2007-01-0007.
(56) Mohammadi, A.; Shioji, M.; Nakai, Y.; Ishikura, W.; Tabo, E. Performance and Combustion Characteristics of a Direct Injection SI Hydrogen Engine. *Int. J. Hydrog. Energy* **2007**, *32* (2), 296–304. https://doi.org/10.1016/j.ijhydene.2006.06.005.
(57) Gersen, S.; van Essen, M.; van Dijk, G.; Levinsky, H. Physicochemical Effects of Varying Fuel Composition on Knock Characteristics of Natural Gas Mixtures. *Combust. Flame* **2014**, *161* (10), 2729–2737. https://doi.org/10.1016/j.combustflame.2014.03.019.

(58) Chen, Y.; Raine, R. A Study on the Influence of Burning Rate on Engine Knock from Empirical Data and Simulation. *Combust. Flame* **2015**, *162* (5), 2108–2118. https://doi.org/10.1016/j.combustflame.2015.01.009.
(59) Ling, Z. Flame Propagation and Autoignition in a High Pressure Optical Engine. phd, University of Leeds, 2014.
(60) Cheng, S.; Saggese, C.; Kang, D.; Goldsborough, S. S.; Wagnon, S. W.; Kukkadapu, G.; Zhang, K.; Mehl, M.; Pitz, W. J. Autoignition and Preliminary Heat Release of Gasoline Surrogates and Their Blends with Ethanol at Engine-Relevant Conditions: Experiments and Comprehensive Kinetic Modeling. *Combust. Flame* **2021**, *228*, 57–77. https://doi.org/10.1016/j.combustflame.2021.01.033.
(61) Mehl, M.; Faravelli, T.; Giavazzi, F.; Ranzi, E.; Scorletti, P.; Tardani, A.; Terna, D. Detailed Chemistry Promotes Understanding of Octane Numbers and Gasoline Sensitivity. *Energy Fuels* **2006**, *20* (6), 2391–2398. https://doi.org/10.1021/ef060339s.
(62) Bradley, D.; Head, R. A. Engine Autoignition: The Relationship between Octane Numbers and Autoignition Delay Times. *Combust. Flame* **2006**, *147* (3), 171–184. https://doi.org/10.1016/j.combustflame.2006.09.001.
(63) Bradley, D.; Kalghatgi, G. T. Influence of Autoignition Delay Time Characteristics of Different Fuels on Pressure Waves and Knock in Reciprocating Engines. *Combust. Flame* **2009**, *156* (12), 2307–2318. https://doi.org/10.1016/j.combustflame.2009.08.003.
(64) Kalghatgi, G. T. Auto-Ignition Quality of Practical Fuels and Implications for Fuel Requirements of Future SI and HCCI Engines; 2005; pp 2005-01–0239. https://doi.org/10.4271/2005-01-0239.
(65) Wang, Z.; Liu, H.; Reitz, R. D. Knocking Combustion in Spark-Ignition Engines. *Prog. Energy Combust. Sci.* **2017**, *61*, 78–112. https://doi.org/10.1016/j.pecs.2017.03.004.
(66) Mehl, M.; Chen, J. Y.; Pitz, W. J.; Sarathy, S. M.; Westbrook, C. K. An Approach for Formulating Surrogates for Gasoline with Application toward a Reduced Surrogate Mechanism for CFD Engine Modeling. *Energy Fuels* **2011**, *25* (11), 5215–5223. https://doi.org/10.1021/ef201099y.
(67) Naser, N.; Sarathy, S. M.; Chung, S. H. Estimating Fuel Octane Numbers from Homogeneous Gas-Phase Ignition Delay Times. *Combust. Flame* **2018**, *188*, 307–323. https://doi.org/10.1016/j.combustflame.2017.09.037.
(68) Naser, N.; Yang, S. Y.; Kalghatgi, G.; Chung, S. H. Relating the Octane Numbers of Fuels to Ignition Delay Times Measured in an Ignition Quality Tester (IQT). *Fuel* **2017**, *187*, 117–127. https://doi.org/10.1016/j.fuel.2016.09.013.
(69) Cheng, S.; Kang, D.; Goldsborough, S. S.; Saggese, C.; Wagnon, S. W.; Pitz, W. J. Experimental and Modeling Study of C2–C4 Alcohol Autoignition at Intermediate Temperature Conditions. *Proc. Combust. Inst.* **2021**, *38* (1), 709–717. https://doi.org/10.1016/j.proci.2020.08.005.
(70) Westbrook, C. K.; Pitz, W. J.; Boercker, J. E.; Curran, H. J.; Griffiths, J. F.; Mohamed, C.; Ribaucour, M. Detailed Chemical Kinetic Reaction Mechanisms for Autoignition of Isomers of Heptane under Rapid Compression. *Proc. Combust. Inst.* **2002**, *29* (1), 1311–1318. https://doi.org/10.1016/S1540-7489(02)80161-4.
(71) Liu, Z.; Chen, R. A Zero-Dimensional Combustion Model with Reduced Kinetics for SI Engine Knock Simulation. *Combust. Sci. Technol.* **2009**, *181* (6), 828–852. https://doi.org/10.1080/00102200902864704.

(72) Goodwin, D. G.; Speth, R. L.; Moffat, H. K.; Weber, B. W. *Cantera: An Object-Oriented Software Toolkit for Chemical Kinetics, Thermodynamics, and Transport Processes*; 2018. https://doi.org/10.5281/zenodo.1174508.
(73) Sarathy, S. M.; Oßwald, P.; Hansen, N.; Kohse-Höinghaus, K. Alcohol Combustion Chemistry. *Prog. Energy Combust. Sci.* **2014**, *44*, 40–102. https://doi.org/10.1016/j.pecs.2014.04.003.
(74) Mehl, M.; Pitz, W. J.; Westbrook, C. K.; Curran, H. J. Kinetic Modeling of Gasoline Surrogate Components and Mixtures under Engine Conditions. *Proc. Combust. Inst.* **2011**, *33* (1), 193–200. https://doi.org/10.1016/j.proci.2010.05.027.
(75) Jaramillo, J.; Zapata, J.; Bedoya, I. D. Interactive Control of Combustion Stability and Operating Limits in a Biogas-Fueled Spark Ignition Engine with High Compression Ratio. *Int. J. Interact. Des. Manuf. IJIDeM* **2018**, *12* (3), 929–942. https://doi.org/10.1007/s12008-017-0446-4.
(76) Han, S. B. Investigation of Cyclic Variations of IMEP under Idling Operation in Spark Ignition Engines. *KSME Int. J.* **2001**, *15* (1), 81–87. https://doi.org/10.1007/BF03184801.
(77) Bade Shrestha, S. O.; Karim, G. A. Considering the Effects of Cyclic Variations When Modeling the Performance of a Spark Ignition Engine; 2001; pp 2001-01–3600. https://doi.org/10.4271/2001-01-3600.
(78) Reaction Design. *CHEMKIN-PRO 15112*; Reaction Design: San Diego, 2011.
(79) Reaction Design. ANSYS Chemkin-Pro 17.2 Theory Manual. **2016**, 414.
(80) Al-Mughanam, T. A. U. Fundamental Characterisation of the Flame Propagation of Synthetic Fuels. Ph.D., University of Leeds, 2013.
(81) Davis, S. G.; Law, C. K. Determination of and Fuel Structure Effects on Laminar Flame Speeds of C1 to C8 Hydrocarbons. *Combust. Sci. Technol.* **1998**, *140* (1–6), 427–449. https://doi.org/10.1080/00102209808915781.
(82) Farrell, J. T.; Johnston, R. J.; Androulakis, I. P. Molecular Structure Effects On Laminar Burning Velocities At Elevated Temperature And Pressure. *SAE Trans.* **2004**, *113*, 1404–1425.
(83) Farrell, J. T.; Weissman, W.; Johnston, R. J.; Nishimura, J.; Ueda, T.; Iwashita, Y. Fuel Effects on SIDI Efficiency and Emissions; 2003; pp 2003-01–3186. https://doi.org/10.4271/2003-01-3186.
(84) Abdi Aghdam, E.; Burluka, A. A.; Hattrell, T.; Liu, K.; Sheppard, C. G. W.; Neumeister, J.; Crundwell, N. Study of Cyclic Variation in an SI Engine Using Quasi-Dimensional Combustion Model; 2007; pp 2007-01–0939. https://doi.org/10.4271/2007-01-0939.
(85) Liu, K.; Burluka, A. A.; Sheppard, C. G. W. Turbulent Flame and Mass Burning Rate in a Spark Ignition Engine. *Fuel* **2013**, *107*, 202–208. https://doi.org/10.1016/j.fuel.2013.01.042.
(86) Roberts, P. J. Fuel and Residual Effects in Spark Ignition and Homogeneous Charge Compression Ignition Engines. Ph.D., University of Leeds, 2010.
(87) Mittal, G.; Sung, C.-J. Autoignition of Toluene and Benzene at Elevated Pressures in a Rapid Compression Machine. *Combust. Flame* **2007**, *150* (4), 355–368. https://doi.org/10.1016/j.combustflame.2007.04.014.
(88) Morgan, N.; Smallbone, A.; Bhave, A.; Kraft, M.; Cracknell, R.; Kalghatgi, G. Mapping Surrogate Gasoline Compositions into RON/MON Space. *Combust. Flame* **2010**, *157* (6), 1122–1131. https://doi.org/10.1016/j.combustflame.2010.02.003.

(89) Agafonov, G. L.; Naydenova, I.; Vlasov, P. A.; Warnatz, J. Detailed Kinetic Modeling of Soot Formation in Shock Tube Pyrolysis and Oxidation of Toluene and N-Heptane. *Proc. Combust. Inst.* **2007**, *31* (1), 575–583. https://doi.org/10.1016/j.proci.2006.07.191.
(90) Richter, H.; Howard, J. B. Formation of Polycyclic Aromatic Hydrocarbons and Their Growth to Soot—a Review of Chemical Reaction Pathways. *Prog. Energy Combust. Sci.* **2000**, *26* (4), 565–608. https://doi.org/10.1016/S0360-1285(00)00009-5.
(91) Frenklach, M. Reaction Mechanism of Soot Formation in Flames. *Phys. Chem. Chem. Phys.* **2002**, *4* (11), 2028–2037. https://doi.org/10.1039/B110045A.
(92) Knyazkov, D. A.; Slavinskaya, N. A.; Dmitriev, A. M.; Shmakov, A. G.; Korobeinichev, O. P.; Riedel, U. Structure of an N-Heptane/Toluene Flame: Molecular Beam Mass Spectrometry and Computer Simulation Investigations. *Combust. Explos. Shock Waves* **2016**, *52* (2), 142–154. https://doi.org/10.1134/S0010508216020039.
(93) Kalghatgi, G.; Babiker, H.; Badra, J. A Simple Method to Predict Knock Using Toluene, N-Heptane and Iso-Octane Blends (TPRF) as Gasoline Surrogates. *SAE Int. J. Engines* **2015**, *8* (2), 505–519. https://doi.org/10.4271/2015-01-0757.
(94) Khan, A. F. Chemical Kinetics Modelling of Combustion Processes in SI Engines. phd, University of Leeds, 2014.
(95) Sarathy, S. M.; Vranckx, S.; Yasunaga, K.; Mehl, M.; Oßwald, P.; Metcalfe, W. K.; Westbrook, C. K.; Pitz, W. J.; Kohse-Höinghaus, K.; Fernandes, R. X.; Curran, H. J. A Comprehensive Chemical Kinetic Combustion Model for the Four Butanol Isomers. *Combust. Flame* **2012**, *159* (6), 2028–2055. https://doi.org/10.1016/j.combustflame.2011.12.017.
(96) Veloo, P. S.; Egolfopoulos, F. N. Flame Propagation of Butanol Isomers/Air Mixtures. *Proc. Combust. Inst.* **2011**, *33* (1), 987–993. https://doi.org/10.1016/j.proci.2010.06.163.
(97) Sileghem, L.; Alekseev, V. A.; Vancoillie, J.; Van Geem, K. M.; Nilsson, E. J. K.; Verhelst, S.; Konnov, A. A. Laminar Burning Velocity of Gasoline and the Gasoline Surrogate Components Iso-Octane, n-Heptane and Toluene. *Fuel* **2013**, *112*, 355–365. https://doi.org/10.1016/j.fuel.2013.05.049.
(98) Wu, F.; Law, C. K. An Experimental and Mechanistic Study on the Laminar Flame Speed, Markstein Length and Flame Chemistry of the Butanol Isomers. *Combust. Flame* **2013**, *160* (12), 2744–2756. https://doi.org/10.1016/j.combustflame.2013.06.015.
(99) Serras-Pereira, J.; Aleiferis, P. G.; Richardson, D. An Analysis of the Combustion Behavior of Ethanol, Butanol, Iso-Octane, Gasoline, and Methane in a Direct-Injection Spark-Ignition Research Engine. *Combust. Sci. Technol.* **2013**, *185* (3), 484–513. https://doi.org/10.1080/00102202.2012.728650.
(100) Aleiferis, P. G.; Serras-Pereira, J.; Richardson, D. Characterisation of Flame Development with Ethanol, Butanol, Iso-Octane, Gasoline and Methane in a Direct-Injection Spark-Ignition Engine. *Fuel* **2013**, *109*, 256–278. https://doi.org/10.1016/j.fuel.2012.12.088.
(101) Gu, X.; Huang, Z.; Wu, S.; Li, Q. Laminar Burning Velocities and Flame Instabilities of Butanol Isomers–Air Mixtures. *Combust. Flame* **2010**, *157* (12), 2318–2325. https://doi.org/10.1016/j.combustflame.2010.07.003.
(102) Vuilleumier, D.; Kim, N.; Sjöberg, M.; Yokoo, N.; Tomoda, T.; Nakata, K. Effects of EGR Constituents and Fuel Composition on DISI Engine Knock: An Experimental and Modeling Study. In *SAE Technical Paper*; 2017.
(103) Kim, N.; Vuilleumier, D.; Sjöberg, M.; Yokoo, N.; Tomoda, T.; Nakata, K. Using Chemical Kinetics to Understand Effects of Fuel Type and Compression Ratio on Knock-

Mitigation Effectiveness of Various EGR Constituents; 2019; pp 2019-01–1140. https://doi.org/10.4271/2019-01-1140.
(104) DelVescovo, D. A.; Splitter, D. A.; Szybist, J. P.; Jatana, G. S. Modeling Pre-Spark Heat Release and Low Temperature Chemistry of Iso-Octane in a Boosted Spark-Ignition Engine. *Combust. Flame* **2020**, *212*, 39–52. https://doi.org/10.1016/j.combustflame.2019.10.009.
(105) Majer, V.; Svoboda, V.; Hynek, V. On the Enthalpy of Vaporization of Isomeric Butanols. *J. Chem. Thermodyn.* **1984**, *16* (11), 1059–1066. https://doi.org/10.1016/0021-9614(84)90134-4.
(106) Svoboda, V.; Charvátová, V.; Majer, V.; Hynek, V. Determination of Heats of Vaporization and Some Other Thermodynamic Properties for Four Substituted Hydrocarbons. *Collect. Czechoslov. Chem. Commun.* **1982**, *47* (2), 543–549. https://doi.org/10.1135/cccc19820543.
(107) Chen, L.; Xu, F.; Stone, R.; Richardson, D. Spray Imaging, Mixture Preparation and Particulate Matter Emissions Using a GDI Engine Fuelled with Stoichiometric Gasoline/Ethanol Blends. In *Internal Combustion Engines: Improving Performance, Fuel Economy and Emission*; Woodhead Publishing, 2011; pp 43–52. https://doi.org/10.1533/9780857095060.2.43.
(108) Bata, R. M.; Elrod, A. C.; Lewandowskia, T. P. Butanol as a Blending Agent with Gasoline for I. C. Engines; 1989; p 890434. https://doi.org/10.4271/890434.
(109) Popuri, S. S. S.; Bata, R. M. A Performance Study of Iso-Butanol-, Methanol-, and Ethanol-Gasoline Blends Using a Single Cylinder Engine; 1993; p 932953. https://doi.org/10.4271/932953.
(110) Sung, C.-J.; Curran, H. J. Using Rapid Compression Machines for Chemical Kinetics Studies. *Prog. Energy Combust. Sci.* **2014**, *44*, 1–18. https://doi.org/10.1016/j.pecs.2014.04.001.
(111) Weber, B. W.; Sung, C.-J.; Renfro, M. W. On the Uncertainty of Temperature Estimation in a Rapid Compression Machine. *Combust. Flame* **2015**, *162* (6), 2518–2528. https://doi.org/10.1016/j.combustflame.2015.03.001.
(112) Atef, N.; Kukkadapu, G.; Mohamed, S. Y.; Rashidi, M. A.; Banyon, C.; Mehl, M.; Heufer, K. A.; Nasir, E. F.; Alfazazi, A.; Das, A. K.; Westbrook, C. K.; Pitz, W. J.; Lu, T.; Farooq, A.; Sung, C.-J.; Curran, H. J.; Sarathy, S. M. A Comprehensive Iso-Octane Combustion Model with Improved Thermochemistry and Chemical Kinetics. *Combust. Flame* **2017**, *178*, 111–134. https://doi.org/10.1016/j.combustflame.2016.12.029.
(113) Westbrook, C. K.; Pitz, W. J. Detailed Kinetic Modeling of Autoignition Chemistry; 1987; p 872107. https://doi.org/10.4271/872107.
(114) Nigam, P. S.; Singh, A. Production of Liquid Biofuels from Renewable Resources. *Prog. Energy Combust. Sci.* **2011**, *37* (1), 52–68. https://doi.org/10.1016/j.pecs.2010.01.003.
(115) Isomäki, R.; Pitkäaho, S.; Niemistö, J.; Keiski, R. L. Biobutanol Production Technologies. In *Encyclopedia of Sustainable Technologies*; Abraham, M. A., Ed.; Elsevier: Oxford, 2017; pp 285–291. https://doi.org/10.1016/B978-0-12-409548-9.10112-5.
(116) Zaharin, M. S. M.; Abdullah, N. R.; Masjuki, H. H.; Ali, O. M.; Najafi, G.; Yusaf, T. Evaluation on Physicochemical Properties of Iso-Butanol Additives in Ethanol-Gasoline Blend on Performance and Emission Characteristics of a Spark-Ignition Engine. *Appl. Therm. Eng.* **2018**, *144*, 960–971. https://doi.org/10.1016/j.applthermaleng.2018.08.057.

(117) Elfasakhany, A. Investigations on Performance and Pollutant Emissions of Spark-Ignition Engines Fueled with n-Butanol–, Isobutanol–, Ethanol–, Methanol–, and Acetone–Gasoline Blends: A Comparative Study. *Renew. Sustain. Energy Rev.* **2017**, *71*, 404–413. https://doi.org/10.1016/j.rser.2016.12.070.
(118) Vlachos, T. G.; Bonnel, P.; Perujo, A.; Weiss, M.; Mendoza Villafuerte, P.; Riccobono, F. In-Use Emissions Testing with Portable Emissions Measurement Systems (PEMS) in the Current and Future European Vehicle Emissions Legislation: Overview, Underlying Principles and Expected Benefits. *SAE Int. J. Commer. Veh.* **2014**, *7* (1), 199–215. https://doi.org/10.4271/2014-01-1549.

TOC Graphic

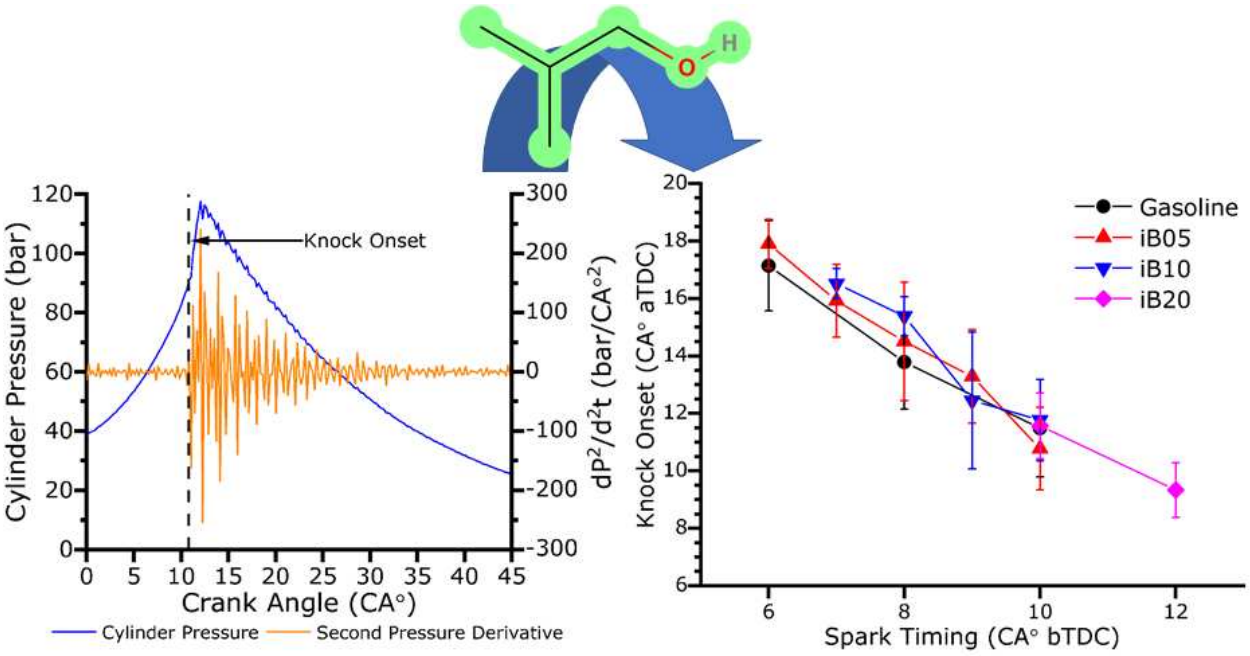
O
H
Cylinder Pressure (bar)
Knock Onset
dP²/d²t (bar/CA°²)
Crank Angle (CA°)
Cylinder Pressure
Second Pressure Derivative
Knock Onset (CA° aTDC)
Spark Timing (CA° bTDC)
Gasoline
iB05
iB10
iB20